VERMONT

AGENCY OF TRANSPORTATION

IDENTIFYING SENSITIVE STRUCTURAL AND HYDRAULIC PARAMETERS IN A BRIDGE-STREAM NETWORK UNDER FLOOD CONDITIONS

Matthew Trueheart, Graduate Researcher
Mandar Dewoolkar, Principal Investigator
The University of Vermont
College of Engineering and Mathematical Sciences

February 2019

The University of Vermont

The information contained in this report was compiled for the use of the Vermont Agency of Transportation. Conclusions and recommendations contained herein are based upon the research data obtained and the expertise of the researchers, and are not necessarily to be construed as Agency policy. This report does not constitute a standard, specification, or regulation. The Vermont Agency of Transportation assumes no liability for its contents or the use thereof.

TECHNICAL DOCUMENTATION PAGE

1. Report No. 2019-02	2. Government Accession No.	3. Recipient's Catalog No.	
4. Title and Subtitle Identifying Sensitive Structural and Hydraulic Parameters in a Bridge-Stream Network Under Flood Conditions		**5. Report Date** February 8, 2019	
		6. Performing Organization Code	
7. Author(s) Trueheart, Matthew (https://orcid.org/0000-0001-6759-3507) Bomblies, Arne (https://orcid.org/0000-0002-3597-2083) Rizzo, Donna (https://orcid.org/0000-0003-4123-5028) Huston, Dryver (https://orcid.org/0000-0002-0957-0574) Dewoolkar, Mandar (PI) (https://orcid.org/0000-0002-8726-0803)		**8. Performing Organization Report No.**	
9. Performing Organization Name and Address College of Engineering and Mathematical Sciences The University of Vermont 33 Colchester Ave. Burlington, VT 05405		**10. Work Unit No.** VTRC 17-3	
		11. Contract or Grant No. RSCH-701	
12. Sponsoring Agency Name and Address Vermont Agency of Transportation (SPR) Research Section One National Life Drive Montpelier, VT 05633		**13. Type of Report and Period Covered** Final Report 2018-2019	
		14. Sponsoring Agency Code	

16. Abstract

The interactions between rivers, surrounding hydrogeological features, and hydraulic structures such as bridges are not well-established or understood at the network scale, especially under transient conditions. The cascading effects of local perturbations up- and downstream of hydraulic structures may have significant and far-reaching consequences, and therefore often cause concern among stakeholders. Tropical Storm Irene resulted in hundreds of millions of dollars in losses to infrastructure and property in Vermont, including damage to or failure of over 300 bridges, and considerable stream restoration efforts thereafter. Climate data show that the state is experiencing more frequent and persistent precipitation events, a trend that is predicted to continue. The replacement or re-design needed for hundreds of existing bridges to meet the rigorous hydraulic standards imposed by extreme flood events is likely not a viable proposition. Moreover, the up- and downstream impacts of modification of a single structure may extend much farther than anticipated, especially in extreme events. This work presents a framework and methodology to perform such a network-level bridge resiliency analysis beyond detailed characterization of site-specific bridge-stream interactions. The stretch of the Otter Creek from Rutland to Middlebury, VT is used as a test bed for this analysis.

A two-dimensional hydraulic model is used to elucidate the impact of individual structures on the bridge-stream network, as well as potential sensitivity to those impacts, during extreme flood events. Depending on their characteristics, bridges and roadways may either attenuate or amplify peak flood flows up- and downstream, or have little to no impact at all. Likewise, bridges may or may not be sensitive to any changes in discharge that result from perturbation of existing structures. Alterations to structures that induce substantial backwaters may result in the most dramatic impacts to the network, which can be either positive or negative. Structures that do not experience relief (e.g., roadway overtopping) may be most sensitive to any network perturbations.

17. Key Words 2D hydraulic modeling; Transient analysis; Extreme flood events; Bridge-river interactions; Bridge resiliency; Flood mitigation	**18. Distribution Statement** No restrictions. This document is available through the National Technical Information Service, Springfield, VA 22161.		
19. Security Classif. (of this report) Unclassified	**20. Security Classif. (of this page)** Unclassified	**21. No. of Pages** 56	**22. Price**

ABSTRACT

The interactions between rivers, surrounding hydrogeological features, and hydraulic structures such as bridges are not well-established or understood at the network scale, especially under transient conditions. The cascading effects of local perturbations up- and downstream of hydraulic structures may have significant and far-reaching consequences, and therefore often cause concern among stakeholders. Tropical Storm Irene resulted in hundreds of millions of dollars in losses to infrastructure and property in Vermont, including damage to or failure of over 300 bridges, and considerable stream restoration efforts thereafter. Climate data show that the state is experiencing more frequent and persistent precipitation events, a trend that is predicted to continue. The replacement or re-design needed for hundreds of existing bridges to meet the rigorous hydraulic standards imposed by extreme flood events is likely not a viable proposition. Moreover, the up- and downstream impacts of modification of a single structure may extend much farther than anticipated, especially in extreme events. This work presents a framework and methodology to perform such a network-level bridge resiliency analysis beyond detailed characterization of site-specific bridge-stream interactions. The stretch of the Otter Creek from Rutland to Middlebury, VT is used as a test bed for this analysis.

A two-dimensional hydraulic model is used to elucidate the impact of individual structures on the bridge-stream network, as well as potential sensitivity to those impacts, during extreme flood events. Depending on their characteristics, bridges and roadways may either attenuate or amplify peak flood flows up- and downstream, or have little to no impact at all. Likewise, bridges may or may not be sensitive to any changes in discharge that result from perturbation of existing structures. Alterations to structures that induce substantial backwaters may result in the most dramatic impacts to the network, which can be either positive or negative. Structures that do not experience relief (e.g., roadway overtopping) may be most sensitive to any network perturbations.

ACKNOWLEDGMENTS

<h1 style="text-align:center">Table of Contents</h1>

1. INTRODUCTION

1.1 Motivation

On August 28, 2011, Tropical Storm (TS) Irene tracked northwards through the Connecticut River Valley and deposited 4-8 inches of rain across Vermont. The storm resulted in unprecedented infrastructure damage, including failure of or damage to over 300 bridges, damage to or closure of over 500 miles of state highway, and 200 miles of state-owned rail. The only comparable event on record in Vermont occurred in 1927 (Anderson et al., 2017a, 2017b, National Weather Service, 2011, State of Vermont, 2012). Research suggests that the state, and the northeastern United States in general, is experiencing a trend of more frequent precipitation events of longer duration, which is anticipated to continue (Guilbert et al., 2015, Horton et al., 2014, Melillo et al., 2014). In this case, infrastructure must withstand more frequent extreme flood events of greater magnitude. However, satisfying the hydraulic demands these floods impose upon all bridges and structures would come at prodigious expense, and is therefore not feasible.

As in much of New England, historical river modifications are ubiquitous in Vermont: of 1,350 stream miles assessed in Vermont, almost three-quarters of these reaches have experienced incision and reduced access to their floodplains (Kline and Cahoon, 2010). A surge in stream restoration and rehabilitation efforts has followed in the wake of TS Irene in Vermont, and other extreme flood events nationwide, although this trend has been ongoing over the past two to three decades. The goals of these projects include mitigating the effects of historical channelization and straightening, dredging and berming, bank armoring, debris removal, and bridge abutment and pier encroachment and constriction (Johnson, 2002, Kosicki and Davis, 2001). Of these, bridges often pose the greatest challenge because they are critical features in transportation and life safety networks, and generally cannot be eliminated in the same way as a historical flood control berm or similar archaic structures.

Bridge crossings are designed to last many decades before replacement, and doing so ahead of schedule is usually cost prohibitive. In the meantime, in the vicinity of hydraulically inadequate crossings, the natural flow regime is interrupted, the channel destabilized, and significant backwaters can develop upstream (Johnson, 2002). These issues can manifest as a considerable hazard under flood conditions. However, structure-induced backwaters also create substantial storage areas that attenuate peak flow magnitude and arrival time downstream, and their elimination can cause justifiable concern from stakeholders (McEnroe, 2006). Thus any alterations to these structures ought to account for these potential far-reaching consequences, ideally striking a balance between mitigating inundation flooding upstream, and attenuation of peak flows downstream.

New or replacement bridges are often designed for bankfull width or greater with minimal piers, which is intended to mitigate hydraulic issues (e.g., constriction, scour) at the bridge site. These bridges

can accommodate the more frequent flood stages, with bankfull discharge generally defined by the Q1.5-Q2.33 flows (67% - 43% annual exceedance probability), without significantly hampering the river's function. More than this, and the river will spill into its floodplain when accessible, and the presence of the bridge and associated infrastructure will begin to influence flow conditions, as longitudinal overbank flow often exceeds channel flow in a large flood. The hazard posed in these situations is dependent upon various characteristics of the bridge-stream intersection, and of course the magnitude and duration of flood stage.

Modern Vermont bridges are designed for Q50 (state-owned) or Q25 (town-owned), and often replace structures built decades before probabilistic theory was applied to flood recurrence intervals. Before this, bridge spans were designed based on ad hoc flood distribution formulae with little or no theoretical basis and/or an engineer's best judgment, although the cost and availability of materials often dictated historical bridge characteristics (Gumbel, 1941). Thus these historical bridges generally consist of short spans with encroaching abutments (Figure 1.1). For those reasons, these bridges are highly susceptible to approach and foundation scour or channel flanking, and their replacements are frequently incomparably different. Among the many potential physical changes, most relevant is the dramatic increase in conveyance capacity of the new bankfull-width structure.
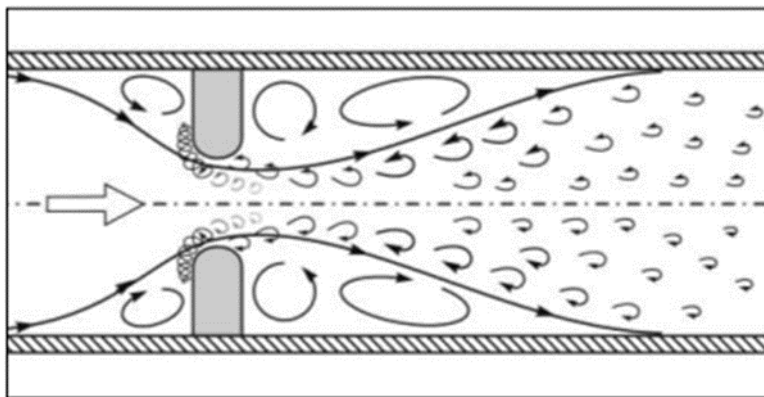
Figure 1.1: Schematic of flow constriction at a bridge (Arneson et al., 2012).

This can alleviate many undesired issues associated with the former constriction, such as scour, backwater flooding, and roadway overtopping, and create a more natural and stable morphological regime in the vicinity of the bridge (Johnson et al., 2002, Johnson 2006, McEnroe, 2006). A consequence of these local benefits is the potential to change hydraulic conditions at property and infrastructure a considerable distance both up- and downstream. This is a frequent concern of stakeholders and should be considered for all new bridge designs and river rehabilitation projects, but is quite difficult to address given the lack of appropriate quantitative methods for assessing transient stream conditions at the watershed scale.

The potentially hazardous localized impacts of floodplain encroachment and bridge constriction on extreme flood events are well-known (e.g., Anderson et al., 2017a, 2017b, Johnson et al., 2002, Lagasse et

al. 2009, 2012). However, analyses are generally limited in scope to the immediate vicinity of the relevant structure or feature, and far-reaching impacts up- and downstream are often not considered or assumed to be negligible. Watershed-scale modeling of large river networks is uncommon due to the substantial labor and computational expense of assessing transient conditions over a vast area. Validation and verification of such a large model is essential if the results are to be at all meaningful, so the ability to calibrate to observed/gauged flows at the inlet and outlet boundaries of the domain is advantageous. Similarly, because of the stochastic conditions that may lead to a 100-year flood (meteorological, hydrogeological, etc.), the characteristics of the associated flow hydrograph are not easily predicted and modeled.

1.2   Objectives

The ability to assess the interdependent resiliency of bridges at variable storm events, including extreme events, at the network level will help prioritize limited resources available for bridge and river rehabilitations, holistic design of bridges, and address stakeholder concerns raised in response to planned bridge and infrastructure alterations. This project built upon the following objectives:

1. Develop a hydrologic/hydraulic model that performs reliable transient analyses of a bridge-stream network to assess the impacts of coupled interactions over a range of design flows.
2. Formulate and implement specific adjustments to the various structures and features in the river corridor to elucidate their respective impacts on the network scale.
3. Perform a sensitivity analysis to examine how specific, localized perturbations to bridges and other structures and features affect up- and downstream bridges, transportation networks, and river corridors. This analysis will enable identification of structural and hydrogeological features of importance, which in turn may be used for quantitative management of infrastructure assets and upgrade prioritization.
4. Develop a methodological framework that can be applied to other bridge-stream networks.

1.3   Background

This section presents a brief review of background information and literature relevant to this research.

1.3.1   Two-Dimensional Hydraulic Modeling

Advances in computer processor power and parallelization over the past decade have made two-dimensional hydraulic modeling more accessible—a high-performance personal computer can perform tasks that previously may have required a large cluster. It has been widely accepted that a 2D hydraulic model is preferable to 1D in most cases because of greater accuracy, resolution, and insight, especially

when flows are not confined to a stream channel (Wu, 2008). Floodplain flow dynamics are essentially neglected in a typical 1D model, but their importance has been increasingly recognized. Development of the models themselves are more forgiving, as a 1D model requires considerable time on-site and the nontrivial process of appropriate cross-section selection (USACE HEC, 2016a,c).

The US Army Corps of Engineers Hydrologic Engineering Center's River Analysis System (HEC-RAS) is recognized as a highly capable software tool for hydraulic modeling, and is freely available. Various other commercial software products are also available; HEC-RAS was chosen for both cost-effectiveness and ubiquitous familiarity to both private firms and government agencies.

A distinct advantage of transient 2D models is the relative ease with which highly informative graphics and animations can be produced and used to communicate complex hydraulic processes to stakeholders who may not be technically inclined.

1.3.2   Local Impacts of Bridges and Infrastructure

The consequences of interruption of natural hydraulic regimes in the vicinity of bridges have been well-established in the literature. Chronic processes such as channel widening, lateral migration, and bed degradation can destabilize the structure over time, regardless of its design. Crossings that are less adequate (more constricting) may experience more acute hazards such as abutment, substructure, or approach scour, which can result in rapid failure of the bridge in flood flows (Lagasse et al., 2009, 2012). Backwaters that form upstream of constricting structures can exacerbate inundation flooding and result in premature roadway overtopping and increased shear stress due to deeper flows in the channel (Johnson, 2002, Johnson et al., 2002, 2006, McEnroe, 2006). As a result, such bridges are often replaced by structures intended to reduce the hydraulic connectivity between the river and bridge, improving local channel stability. This may occur either at the end of the previous structure's design life, or following its partial or complete failure.

In the meantime, various countermeasures may be employed to mitigate scour at a bridge, such as installation of cross-vanes, J-hook weirs, sacrificial piles, or bank armoring. Flow-altering devices are generally preferable to rip-rap, as they tend to diffuse energy rather than deflecting it. However, these are usually more expensive to design and install, and ensuring their stability in flood conditions is more difficult. Bank armor is highly effective at channel stabilization where it is installed. However, excess energy is redistributed at the up- and downstream extents of the armoring, leading to bank undercutting and failure, and increased hazard of flanking flow. Thus, more rip-rap is necessary, as erosion must perpetually be "chased" ever further away from the protected structure (Johnson, 2002).

A river channel is most stable under natural conditions, though this is a dynamic equilibrium in which both acute and chronic geomorphological processes continuously alter flow dynamics at a given location. Unfortunately, (re-)establishment of the natural flow regime is often fundamentally in conflict

7

with the design objectives of a crossing structure. For example, permission of unrestricted channel migration for the lifetime of a bridge may necessitate a clear span of the entire floodplain, which is seldom practical financially.

1.3.3 Network-Scale Impacts

A study by the Kansas Department of Transportation (McEnroe, 2006) exploring the downstream effects of enlarging a constricting culvert or bridge concludes that "if the peak flows through the existing structure are affected by detention storage, enlargement of the structure will increase the peak flows and might also increase channel erosion. The peak flow through the enlarged structure will also occur sooner, which may be significant in an analysis of downstream impacts." The implication is a relationship between a reduction in backwater storage and increased downstream peak flows. This is a fairly intuitive observation, but does not necessarily apply in all cases, as will be presented in this study.

The extent of the area of influence of these bridges under various flow conditions is difficult to assess quantitatively, and may in some cases only be determined when they are removed or replaced. For example, removal of a 200-year old, 13 foot high dam on a low-gradient reach of the Ashuelot River in Swanzy, NH revealed that the dam's backwater extended over six miles upstream under normal flow conditions, and drawdown subsequent to removal reactivated an upstream glaciofluvial boulder deposit as a grade control (Gartner et al., 2015). While here we are mostly concerned with bridges and right-of-way berms, in the context of the Otter Creek study area, bridges and their associated roadways essentially act as a series of low-head dams during floods. Further, this is a fine example of both the far-reaching effects of even a small hydraulic structure, and the potentially unanticipated regime change imposed by geologic features that had historically been rendered ineffective. This of course can work the other way—in a situation where the hydraulic control imposed by a hydrogeological or other natural feature is far more substantial than those of a proximal structure (e.g., a bridge spanning a gorge or valley pinch-point), adjustments to that bridge may not significantly affect the network.

Literature searches reveal a lack of quantitative assessments of bridge-stream network interactions. This is surprising given the current emphasis on watershed-scale resiliency research (e.g., Abdulkareem and Elkadi, 2018, Cheng et al., 2017, Kline and Cahoon, 2010). Michielsen et al. (2016) leverage watershed and transportation infrastructure data to estimate the vulnerability of bridges to flooding damage based on statistical models, though these assessments focus on watershed response to flooding as a whole, not interactions within that network that may affect response of individual structures as well.

2. STUDY AREA

The Otter Creek drains 945 mi^2 as it flows 112 miles through west-central Vermont, ultimately discharging into Lake Champlain. The USGS operates flow gauges at both Rutland and Middlebury, VT,

some 46 miles apart, which are the bounds of this study's model, and have been in operation since 1928 and 1903, respectively. Five major tributaries empty into this stretch of the Otter Creek. The main channel is spanned by 14 roadway bridges, four of which are historic covered bridges, as well as eight bridges of the Vermont Railway (VTR) Northern line, which runs through the Otter Valley, for a total of 22 structures. Additional infrastructure in the Otter's floodplain on this stretch includes 75 miles of town- and state-owned highway, 30 miles of state-owned rail, several overflow bridges, and more than 100 culverts. A hydropower station operates at Proctor Falls, 7.5 river miles (12 km) downstream of the Rutland gauge (Figure 2.1).

Overall, the Otter is a shallow-slope (<1%), meandering river, and generally has access to its substantial, broad floodplain (Rosgen type E5-E6). Massive storage is available in these floodplains, a phenomenon that is enhanced by the constrictions and backwaters imposed by bridges and elevated rights-of-way traversing the plain. These features can be imagined to be acting as low-head dams or weirs, with bridges and culverts for gates and roadway overtopping acting as emergency spillways.

Because of these characteristics, it is anticipated that in a bridge-stream network with high spatial hydraulic connectivity, such as the Otter Creek, the interactions between structures will be maximized, yielding a conservative analysis. The presence of up- and downstream gauges, consistency of those gauges' records, relative accessibility of the river, availability of high-water surveys, and variety of bridge/roadway constructions in the river corridor make the Otter an excellent location to develop the proposed methodology. Further, the Otter Creek's appreciable floodplain access makes it one of the healthier river corridors in Vermont. Many of the river's features (e.g., wetland complexes, riparian buffers, minimally restricted lateral floodplain access) are targets of river rehabilitation projects elsewhere, which makes Otter Creek especially relevant and helps distinguish the impacts of bridges, infrastructure, and hydrogeological features from the impacts of other development.

The USGS Streamstats program uses watershed hydrologic characteristics to estimate flood frequency and magnitude at a specific site based on regional regressions developed from gauged rivers (Olson, 2014). In Vermont, these regressions are more applicable to steeper mountain streams, and grossly overestimate flows in the Otter Creek; for example, only once in 115 years of observations at the Middlebury gauge has flow exceeded Streamstats' estimated 2-year flood at this location. Further, rather than attenuation of downstream peak flows due to floodplain and/or backwater detention, regressions indicate an increase in peak discharge from bridge to bridge downstream. This is shown in Table 4.3 in Chapter 4.
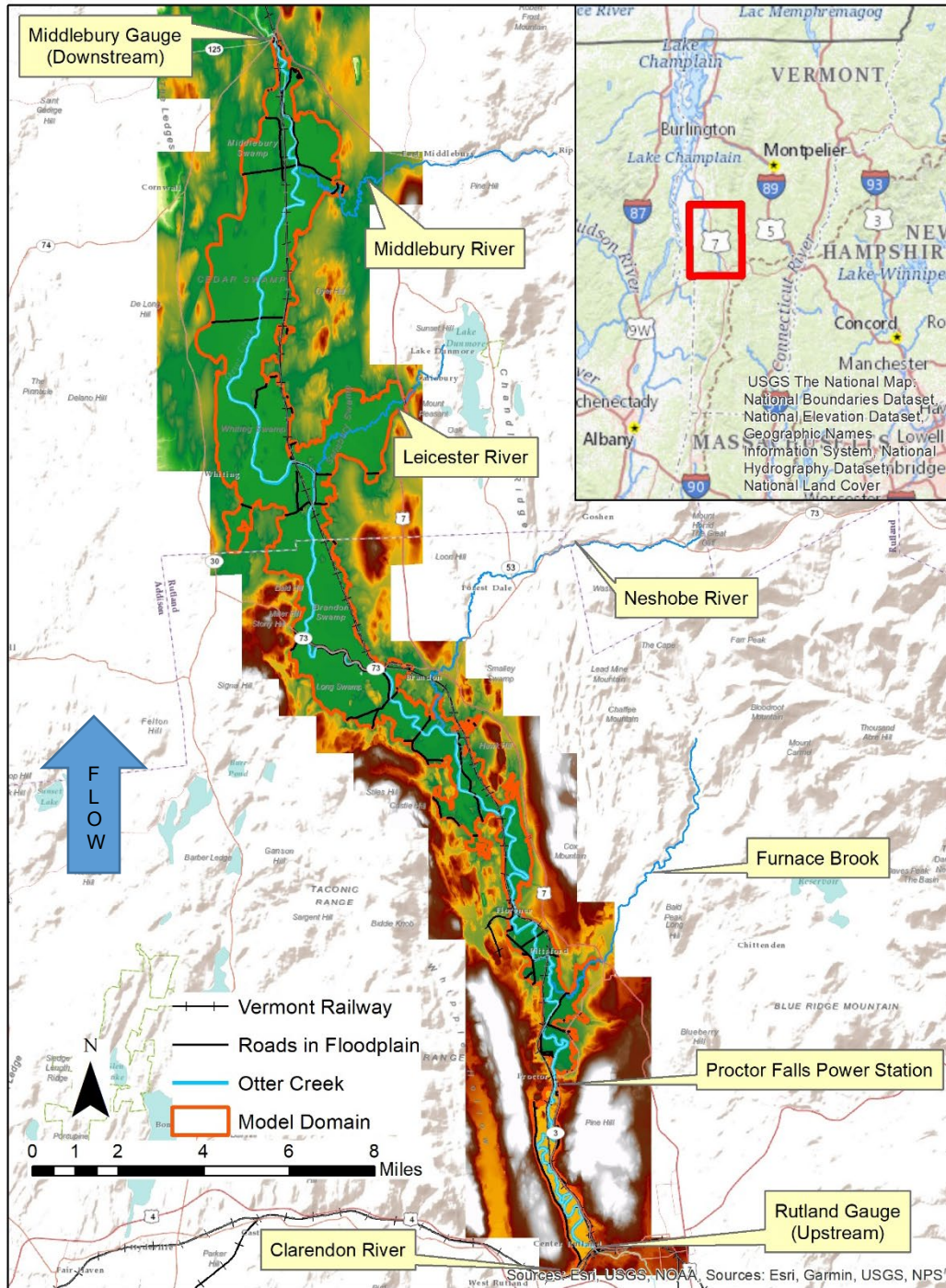
Figure 2.1: Map of Otter Creek Study area, showing gauge locations, tributaries, model domain, and rights-of-way in the floodplain.

The combined wetland and floodplain complexes in the Otter Valley, in economic terms, provide an estimated $100,000 - $450,000 in flood mitigation services to the downstream town of Middlebury annually, and reduced damage in TS Irene by 84% - 95%, or $400,000 - $1,240,000 (Watson et al., 2016).

These wetlands consist of hundreds of interconnected acres, occasionally interrupted by infrastructure, many miles upstream of Middlebury, yet their effect there is undeniable. TS Irene is the flood of record (88 years) at the Rutland gauge, at 15,700 cubic feet per second (cfs). In Middlebury, 4 days later, the peak arrived at 6,180 cfs, ranking only 12th in annual peak flow over a 101-year record (two of the 11 higher-ranking flows occurred before installation of the Rutland gauge). Without the Otter's floodplain access a considerable distance upstream, TS Irene may have posed a much greater risk to Middlebury and the five hydro-power stations downstream.

This sort of hazard attenuation—or intensification—over dozens of miles is impossible to assess under steady-state conditions, so we sought to understand quantitatively the dynamic interactions between a river and its surrounding infrastructure under high-risk, transient conditions. By identifying critical structural and hydrogeological features in a bridge-stream network, a network-level infrastructure resiliency analysis is possible. Such analysis may help prioritize limited resources available for bridge and river rehabilitations, holistic design of bridges, and address stakeholder concerns raised in response to planned bridge and infrastructure alterations.

3. METHODOLOGY

3.1 Data Collection

All field data were collected in June of 2018. The following subsections describe the details of data gathered, and methods used for synthesis.

3.1.1 Terrain Model

Relevant tiles from the Vermont Center for Geographical Information's hydro-flattened Lidar scans of Addison (2012, 1.6m post-spacing) and Rutland counties (2013-2015, 0.7m post-spacing, downsampled to 1.6m) were downloaded and mosaicked into a digital elevation model (DEM) of the Otter Creek basin. This DEM provided the terrain boundary condition for the two-dimensional HEC-RAS model (5.0.5). The effects of water surface scattering on the Lidar scan are accounted for by repeated georeferenced sonar soundings of the channel bottom. Bridge locations required additional adjustment because their decks are somewhat arbitrarily deleted from the Lidar scan during hydro-correction post-processing, resulting in inaccurate span lengths and abutment geometries, and elimination of any piers.

Many relevant bridge geometry parameters are available from VTrans long structure asset inventories, including number of spans and their lengths. However, key features such as pier and abutment geometries and low-chord elevations were not available, and were measured in the field as part of this project. The terrain model was updated based on these additional data. It should be noted that these corrections are constrained by the 1.6-meter resolution of the terrain model, which may introduce small errors, but are nonetheless an improvement over the raw Lidar terrain. Further, low-chord elevations were measured relative to roadway elevations, and their accuracy is therefore contingent upon the accuracy of the Lidar-derived elevations of the associated approach.

3.1.2 Side-Imaging Sonar

A Humminbird Helix 7, recreational-grade "fishfinder," sonar unit with a built-in GPS receiver was used for a bathymetric survey of the Otter Creek by both powerboat and canoe. Side-imaging scans can be corrected for incidence angle and range to create a detailed bathymetry model, but yaw and roll of the watercraft—especially the canoe—precluded the utility of these. Instead, a minimum of two longitudinal passes on each reach, with pings recorded at 10- to 15-foot intervals, resulted in a total of 29,000 soundings over the relevant 46 miles of river channel.

Differences in river stage between the Lidar and sonar scans were corrected based on water surface elevation (WSE) relative to the Vermont Railway grade at the time of the respective collection: for the Lidar scan, this is measured directly on the terrain model; for the sonar scan, this is laser-measured from the water surface to the underside of the rail. Level spans and fairly consistent spacing of rail bridges

allowed this sufficiently accurate measurement for each day of sonar data collection. The difference is added or subtracted, as appropriate, from measured water depth on the relevant reach (Figure 3.1).
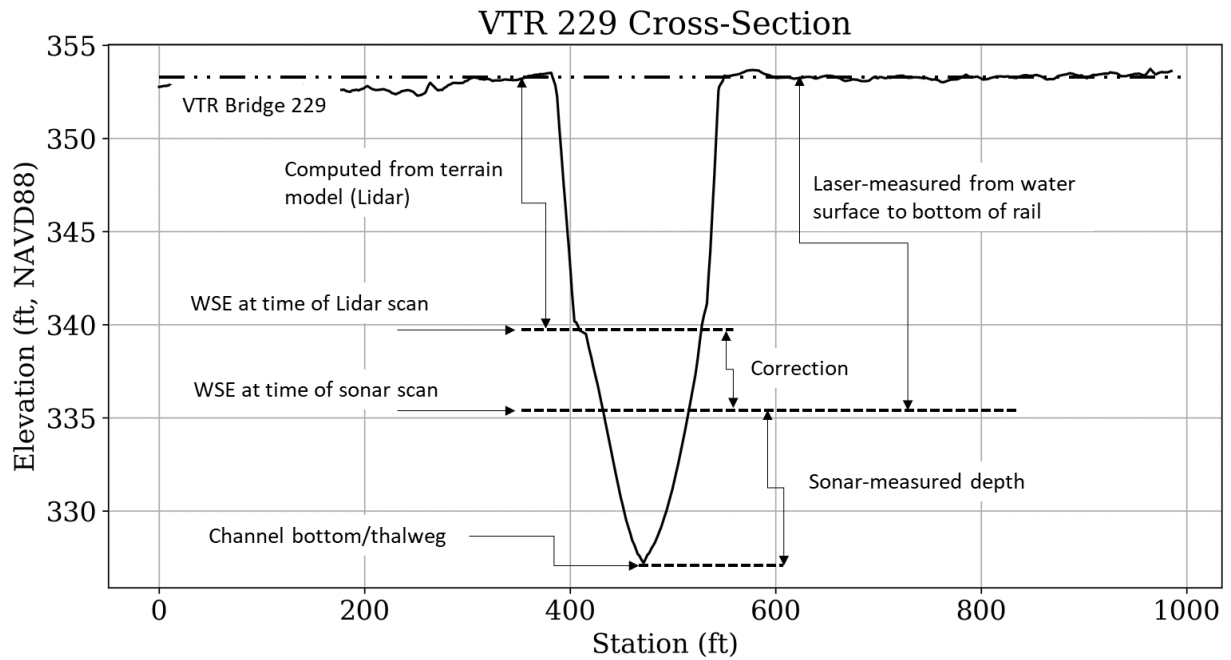
Figure 3.1: Correction of sonar-measured depth for river stage at time of scan.

A zero-depth contour was traced along the water surface-streambank interface in GIS, and converted to points at 1m intervals. An interpolation between these and the corrected depths yields a sufficiently accurate channel bathymetry model that can be merged with the original terrain into a single DEM. This correction accounts for an additional 3,000 acre-feet (10^9 gal, 3.5×10^6 m^3) of volume in the channel. Sounding and interpolation methods result in a fairly smooth bathymetric model that does not incorporate all intricacies of the channel bottom. However, the depth-averaged numerical scheme employed by the HEC-RAS 2D solver does not require capturing every detail of bed roughness; rather, only an accurate elevation-volume relationship for a given computational cell is necessary (USACE HEC, 2016b). Agreement between surveyed cross-sections (where available) and the Lidar/sonar hybrid terrain is strong (Figure 3.2).
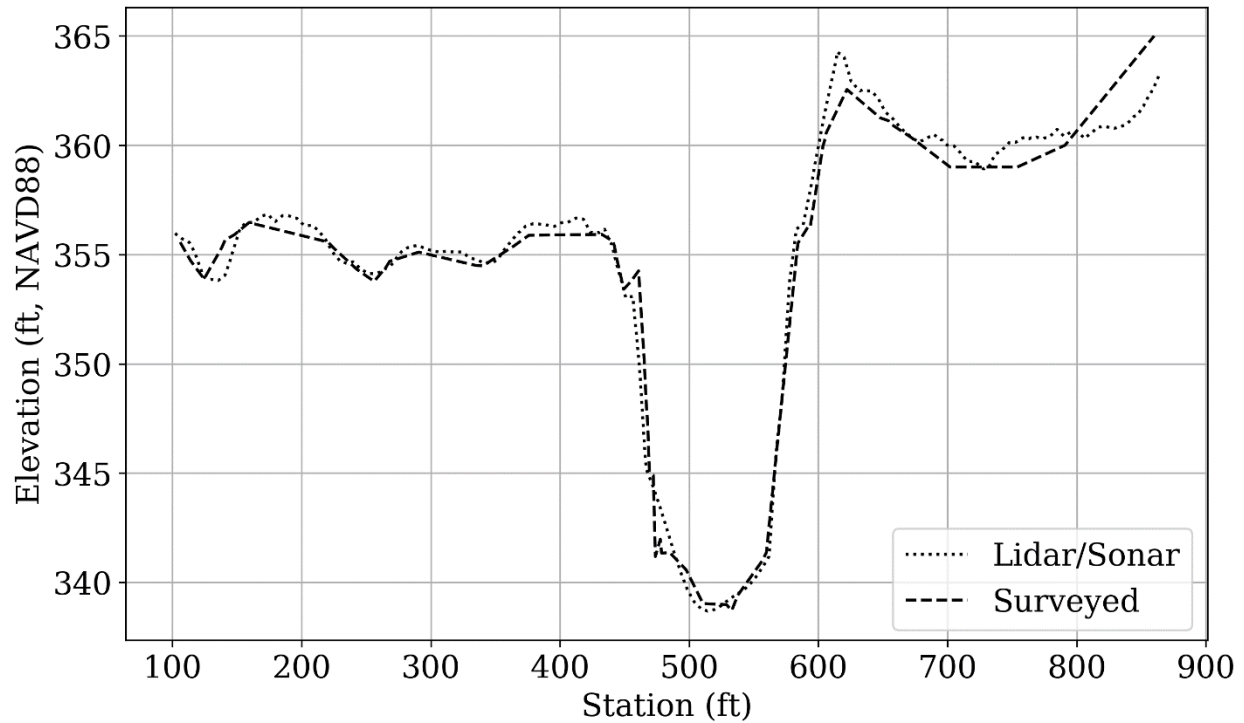
Figure 3.2: Comparison of surveyed and Sonar/Lidar DEM-derived cross-sections near VTR Bridge 219.

3.2 Numerical Model

All hydraulic models were developed using the US Army Corps of Engineers' Hydraulic Engineering Center's River Analysis System (HEC-RAS) software v. 5.0.5 (USACE, 2018). Analyses were performed in SI/metric units for consistency with input data formats; results are converted to standard units.

3.2.1 Geometry and Computational Domain

Two 2D computational domains were developed: the first extends from the gauge at Rutland to the gauge in Middlebury; the second, from Proctor Falls (7.5 miles downstream of Rutland gauge) to the gauge in Middlebury (Figure 2.1). The two geometries are identical in their intersection, but the latter has 13,000 fewer computational nodes and does not require computation of flows through the Proctor Falls power station. For the sensitivity analysis, each magnitude flood event is simulated once on the larger domain, and the hydrograph calculated through the dam provides the upstream boundary condition for subsequent simulations of that flood on the smaller domain. This hydrograph accounts for changes between Rutland and Proctor as well as the confluence of the Clarendon River on this reach. Additionally, the domain is reduced by 10%; the number of inflow boundary conditions is reduced by one; and the computational

expense associated with routing the hydrograph through the dam gates and spillways, as well as nearly two dozen upstream culverts, is eliminated.

Nominal node spacing in the model is set to 82 ft (25 m), with local simplification (164-328 ft, 50-100 m) in broad floodplains, and refinement (49 ft, 15 m) extending 250 ft (75 m) on each side of the channel centerline and in the vicinity of hydraulic structures, over a 40 mi^2 (100 km^2) domain in the Otter Valley. Mesh break lines define channel banks, roads and railroads (both active and abandoned), berms, and other at-risk structures, such as the Proctor wastewater treatment facility. These prevent "flow through" that occurs when a single computational cell straddles such a feature.

More than 100 hydraulically connected culverts were initially incorporated into the model. Sufficient data were available for highway culverts maintained by town and state agencies; the many archaic culverts associated with agricultural activity or abandoned infrastructure were measured in the field and modeled as well as possible (e.g., there are no FHWA culvert charts for an old rail tanker car with the ends cut off). Railroad asset inventories currently have no data on any culverts of the VTR Northern line in the Otter Valley. Where accessible from the river, these culverts were measured in the field; otherwise, their locations were identified from the Lidar terrain and characteristics were approximated. No analysis is performed on the latter set; they are included only for the sake of accurately mapping inundation extents. A total of 22 culverts with diameters of one foot or less were subsequently excluded due to their low conveyance capacity as well as their computational burden (simulation time is reduced by approximately 12% with these culverts excluded). Solutions were not appreciably altered due to these simplifications.

Bridge foundations and substructures are incorporated into the terrain model. This required minor adjustment to Lidar-measured abutment geometry as well as addition of any piers. Computational node and cell face positioning were carefully oriented so that these substructural features are simulated as obstructions to flow, rather than simply volume displacement in a single cell.

3.2.2   Boundary Conditions

Six inflow boundary conditions are applied to the domain. For model calibration, observed discharge from Tropical Storm Irene at the Rutland gauge (15 min) is used as the main upstream inflow boundary condition. Five ungauged tributary streams are also modeled: Furnace Brook, and the Clarendon, Neshobe, Leicester, and Middlebury Rivers. Tributary inflow hydrographs are estimated by their respective watersheds' proportional areas as compared with the gauged, hydrologically comparable New Haven River, which meets the Otter Creek just downstream of the outflow boundary of the domain. Peak magnitudes of these estimates are confirmed by comparison with USGS Streamstats data, which are far more reliable for these steeper mountain streams than for the Otter itself, and estimates correlate well with recurrence intervals computed for the New Haven River gauge (Olson, 2014). Estimated hydrographs for the Leicester

River are probably flashier than reality because of storage in Lake Dunmore, approximately four miles upstream of its confluence with Otter Creek.

A normal depth outflow boundary condition is applied at the Middlebury USGS gauge, just upstream of the falls in Middlebury. Initial conditions were generated by the software by running a steady-state simulation using the initial values of the inflow boundary conditions until these flows reached the outlet boundary. This takes approximately 100 hours of simulated time.

3.2.3   Numerical Scheme and Computational Parameters

HEC-RAS may employ either one of two unsteady equation sets: the full shallow water (SW) equations (St. Venant, momentum) or the diffusion wave approximation thereof (DSW). The HEC-RAS Reference Manual and 2D User's Manual describe these computational schemes in detail, their advantages and drawbacks, and appropriate selection criteria based on anticipated flow dynamics in the domain (USACE HEC, 2016b, c). The diffusion wave set is used here rather than the full momentum equations because of the overall low celerity in the domain, dominance of barotropic pressure gradients and bottom friction in flow governance—as opposed to turbulence or Coriolis effects—as well as the considerable speed and stability advantages of the former compared to the latter. In addition to requiring more flops per iteration, the full SW equations also generally require a denser mesh for stability, which essentially precludes their use in simulating a domain this size for this duration (with available computing power).

An adjustable timestep is employed, with $\Delta t_{min} = 10$s and $\Delta t_{max} = 40$s. The timestep is controlled by satisfaction of a threshold Courant number, 4.0. This is technically in violation of the Courant-Freidrichs-Lewy (CFL) condition for convergence of an explicit finite-difference numerical solution to any hyperbolic partial differential equation, including those employed here, but the semi-implicit numerical scheme of the HEC-RAS 2D DSW solver can accommodate Courant numbers as high as 5.0 without loss of stability (Courant et al., 1928, USACE HEC, 2016b). That being said, Courant numbers >1.0 (but <2.0) are encountered almost exclusively in a handful of cells at the tailwater of the Proctor Falls dam. Otherwise, C_{max} in the domain is <1.0. A maximum of 15 iterations without improvement are permitted; convergence was rarely achieved beyond this threshold.

Seven hundred hours of simulated time (~1 month) is sufficient to capture the full storm hydrograph at the downstream boundary of the domain; data are written every 15 minutes.

3.2.4   Synthetic Unit Hydrograph Development

To simulate various flow events, a synthetic unit hydrograph was developed for the Rutland gauge location on the Otter Creek. This requires both shape and scaling parameters, which were derived from the gauge record and estimated rainfall annual exceedance probability (AEP). A log-Pearson Type III

distribution was applied to the 90 years of gauge record at Rutland (Figure 3.3), from which the magnitude of relevant AEP events were computed, and tabulated in Table 3.1.
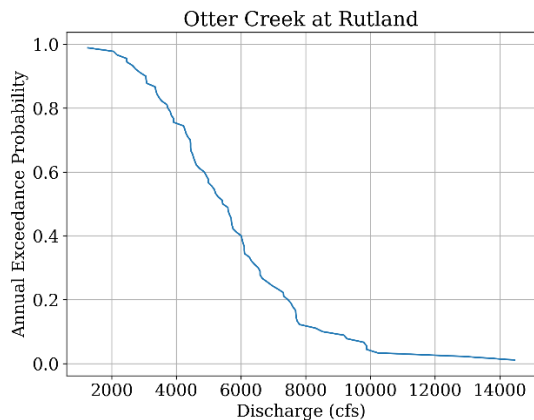
Figure 3.3: Flow duration curve for Rutland gauge based on 90 years of record. Relevant AEP are tabulated in Table 3.1.

Table 3.1: Magnitude of selected recurrence-interval floods at the Rutland gauge on the Otter Creek.

Recurrence Interval (years) / AEP (%)	Peak Discharge (cfs)
500 / 0.2%	15,600
200 / 0.5%	14,000
100 / 1.0%	12,900
50 / 2.0%	11,700
25 /4.0%	10,500
10 /10.0%	8,800

TS Irene resulted in peak flows through the Rutland gauge of 15,700 cfs, indicating a 500-year event in terms of discharge magnitude. However, this rating does not account for the total mass of the flow event—for example, a 12-hour storm and a 2-day storm may produce the same peak flows, but the total flow volumes over the two events will be different. The briefer storm's sharper flood wave will experience more substantial attenuation as it moves through the watershed because a larger proportion of its total volume can be detained in storage at a given time. For example, peak flows at the downstream gauge in Middlebury were only a 10-year event for TS Irene, while the far more substantial synthetic 500-year flood results in a 100-year flow in Middlebury. Spring/snowmelt floods are the only high-flow events that crest at a greater peak in Middlebury than in Rutland.

The Middlebury gauge has been in operation about 20 years longer than Rutland, and the peak flow distribution is (relatively) skewed by major floods in 1913 and 1936, and the Flood of 1927, which were not captured by the Rutland gauge. This affects the AEP classification of a given flood, but does not explain

the substantial attenuation of peak discharge observed during TS Irene, and the surprisingly comparable Flood of 1938 (Table 3.2).

Table 3.2: Comparison of TS Irene and Flood of 1938.

Flood	Q_{pk} Rutland (cfs)	Q_{pk} Middlebury (cfs)	Ratio
Sept. 1938	13,700	6,630	0.48
Aug. 2011 (TS Irene)	15,700	6,180	0.39

The two dams that regulate flows on the relevant stretch of the Otter Creek (Rutland Center Falls just upstream, and Proctor Falls within the domain) were both constructed before either gauge, so these impacts are captured in the entire record. Both are hydro-power stations, have limited storage capacity (110 and 460 ac-ft), and are not able to perform significant flood control function. Land-use has undoubtedly changed over the decades; widespread abandonment of agricultural activity in Vermont in the mid-1900s presumably had a substantial impact on watershed response to flooding, but there are insufficient data and far too many complicating factors to support this hypothesis. Differences in the number and characteristics of bridges and engineered features may be similarly responsible for any changes, but, again, the stochastic conditions that produced the two floods cannot be reconciled with this supposition. Ultimately, it is the vast wetland and floodplain complexes in the Otter Valley that are responsible for the overwhelming majority of flow attenuation observed at the Middlebury gauge, which has not changed substantially over the years.

With this in mind, there are several important upshots. First, the Rutland gauge record does not contain spurious reductions in peak flows seen on other Vermont rivers following installation of flood control dams, and it is therefore appropriate for return-interval analysis in this regard. Second, watershed response is drastically different under snowmelt/frozen ground/rain-on-snow conditions than for a strictly rainfall-induced event. This study is focused on the latter scenario, so it is important to note that profoundly disparate results than those presented are possible, depending on antecedent conditions. Third, it is impossible to predict the exact circumstances that will result in a given flood event, so modeling network response to a specific peak flow through the Rutland gauge is more practical than attempting to simulate response to a specific rainfall event.

To that end, a synthetic unit hydrograph was developed based on observed discharge during 14 non-snowmelt, high-flow events from 1994 to 2017 at the Rutland gauge. These hydrographs were nondimensionalized and aggregated to yield a unit hydrograph that represents the average shape of flood flows through the gauge (Figure 3.4). Individually, there are myriad differences between the input hydrographs, ranging from subtle to substantial. However, because the exact runoff response is dependent on the combination of dozens of complex, unpredictable factors, the development of a reasonable "typical"

synthetic hydrograph is sufficient for this analysis. The unit hydrograph is scaled to the relevant peak flows derived from the return-interval analysis, and total mass of a 2-day rainfall event of the relevant recurrence interval (Perica et al., 2015). These are intended to represent some of the most substantial flooding possible (within reason) for a given peak flow magnitude, intended to marginalize floodplain storage and propagate high discharges through the entire domain. Ungauged tributary flow hydrographs were similarly constructed based on estimated peaks from the USGS Streamstats program (Olson, 2014).
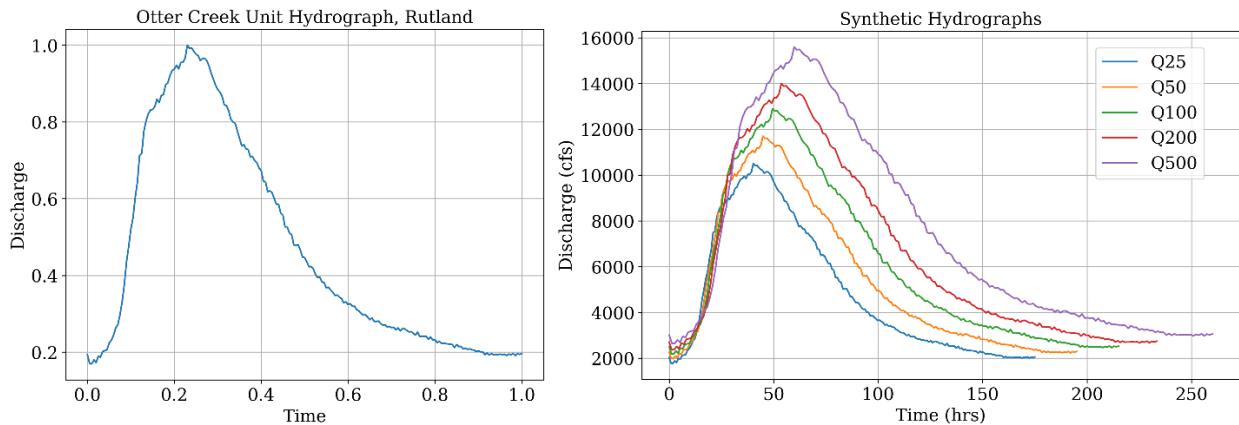
Figure 3.4: Dimensionless synthetic unit hydrograph for Rutland gauge (left), scaled to relevant AEP flood events (right).

3.2.5 Calibration

Because this model is intended for simulating extreme flood scenarios, TS Irene is an excellent event to leverage for model calibration for several reasons. First, it is the largest flood for which instantaneous data are available at the Rutland gauge which enables floodplain/overbank hydraulic properties to be properly calibrated. Further, the Lidar scans for the terrain model were flown within two years of TS Irene, and a great deal of information for the event is available, beyond just the gauge records. These gauges are invaluable. Observed flows are used as boundary conditions, and roughness parameters are adjusted so that modeled outflows agree with observations at the downstream gauge.

Manning's roughness values (Table 3.3) are applied based on land cover types identified by the 10m-resolution (~33 ft) 2011 National Land Cover Database (NLCD) (Homer et al., 2015). Typical values from the literature are used initially, and adjusted based on conditions observed in the field and remotely sensed imagery, or overridden where necessary (e.g., land cover type is incorrectly identified in the NLCD) (Acrement and Schneider 1987, 1989, Chow 1959). Flooding in the Otter Valley from TS Irene occurred for several days between the end of August and early September, 2011. At this time, natural floodplain and riparian vegetation is near its densest, and row crops have matured and are still standing. Hay fields may

be at various lengths depending on landowners' practices or schedules, but overall, the model is calibrated to relatively high-roughness overbank conditions.

A Nash-Sutcliffe efficiency rating of 0.78 was achieved for TS Irene at the downstream gauge/boundary location, with peak flow magnitude and arrival time within 100 cfs and 4 hours, respectively (Nash and Sutcliffe, 1970). Further, the USGS conducted extensive high-water mark surveys in the Otter Valley and elsewhere in Vermont following TS Irene (Medalie and Olson, 2013). Twenty of these are located in the model domain, providing additional locations for calibration besides those at the domain boundaries.

Correlation of modeled water surface elevations with observed high-water marks is generally strong, however modeled values tend to consistently overestimate peak water surface elevations by 4"-8" (10-20 cm) or more. This is presumably due at least in part to inherent errors in Lidar data collection and processing, but largely a result of overestimated terrain elevation due to dense vegetation in floodplain wetlands. Hodgson et al. (2005) report absolute errors between Lidar DEM and surveyed benchmark elevations of approximately 4"-10" (10-25 cm), depending on land cover, for a leaf-off scan. These errors are less in magnitude in areas without vegetation cover, such as road surfaces. Thus it is possible that roadway overtopping is initiated in the model either earlier than in reality, or even when it does not occur at all, because of spurious volume displacement by the terrain model. This is somewhat concerning, but is presumably mitigated to some degree by the fact that direct rainfall on the domain (5"/Q25 to 9"/Q500), which would otherwise temporarily occupy some of this volume, is neglected.

Table 3.3: Calibrated roughness values

Cover Type		Manning's n	% Total Area
Barren		0.04	2.0%
Cultivated Crops		0.065	10.7%
Deciduous Forest		0.12	2.6%
Developed	High Intensity	0.04	0.5%
	Medium Intensity	0.05	1.1%
	Open Space	0.04	1.4%
Emergent Wetlands		0.12	12.0%
Evergreen Forest		0.13	1.2%
Grassland		0.06	0.3%
Mixed Forest		0.11	0.4%
Pasture/hay		0.06	17.1%
Shrub/scrub		0.1	1.6%
Woody Wetlands		0.13	49.0%
Otter Creek Channel		0.04-0.06	

Simulations using the calibrated terrain roughness values with the non-bathymetrically corrected terrain model results in underestimated peak discharge at the model's outlet boundary by about 1,000 cfs, or about 16% of the peak value for TS Irene. This reduces the Nash-Sutcliffe efficiency rating to 0.42, and highlights the value of conducting the sonar survey of the channel. If the raw lidar terrain model was used exclusively, roughness parameters would likely have been calibrated to different—and less accurate— values in order to improve ersatz model efficiency. Without the additional cross-sectional flow area provided by the sonar data, velocity and discharge through bridges may be underestimated by as much as 37% and 40%, respectively, and WSE overestimated by as much as 1.1 feet. These discrepancies, which substantially affect this study's most fundamental results, would occur even if overbank roughness values were differently calibrated. Because of the Otter Creek's nonnegligible depth, the accuracy gained by sounding the channel more than justifies the additional labor it requires.

3.2.6 Verification and Validation

Mesh convergence was verified by simulating TS Irene using uniform 164-, 100-, 65-, and 50-foot (50, 30, 20, 15 m) node spacing in the domain, with all appropriate break lines. Computational timesteps were adjusted in order to satisfy the Courant condition for each geometry. The final geometry was constructed on an 82' (25m) grid, with a 50' (15m) refinement region within, and extending 148' (45m) beyond, the channel. Resolution was downsampled to 164-328 ft (50-100 m) in broad areas of floodplain and swamp around the margins of the domain. A minimum of three cells span the channel. Solutions are virtually identical to the finest-resolution uniform mesh tested, and compute in roughly 20% the time.

A minimum timestep of 5 s was compared to that of 10 s on this geometry, which reduced the number of iterations required for numerical convergence at intermediate timesteps, but nearly doubled the total simulation time without significantly altering the solution. Courant numbers reduced (necessarily) across the domain, but the expense of strictly satisfying the CFL condition for the <10 out of 124,000 nodes where it is momentarily violated is not economical. All simulations are therefore computed with $\Delta t_{min} =$ 10s.

Several spurious artifacts exist in the domain, generally due to computational instabilities that occur when water surface elevation (WSE) is at or just above culvert invert elevations in adjacent cells, when pressure flow is first initiated in culverts, or when uncharacteristically high velocities are encountered at the onset of roadway overtopping. These manifest as an individual timestep wherein unrealistically high velocities are passed across a cell face, but stability is re-established after no more than two Δt, and no appreciable discrepancies are observed.

Numerical integration of modeled versus observed flows through the Middlebury gauge and analysis of National Weather Service rainfall totals for TS Irene show that the total modeled flow volume through the domain is deficient by almost exactly the volume of rainfall that fell on the domain. This indicates that the estimated tributary flow volumes are reasonably accurate, if not precisely timed.

Flooding in the spring of 2018 was simulated and the results compared well with both provisional observed gauge data (0.73 Nash-Sutcliffe rating), as well as time-indexed field observations of WSE at 15 locations along some 20 miles of river from Pittsford to Cornwall from April 27 to May 1, 2018. Flood crests were on April 26 (2,720 cfs) and May 5 (3,550 cfs) at the Rutland and Middlebury gauges, respectively. These flows are far less than the floods of interest, but are sufficient to inundate a substantial area of floodplain and overtop several roads, making the event useful for confirming model fidelity. This was also the only event exceeding bankfull experienced by the Otter Creek during this study's timeframe. Modeled depths uniformly overestimated observations within one foot.

4. SENSITIVITY ANALYSIS

4.1 Assessed Perturbations

In order to test the effects of localized adjustments to bridges on up- and downstream structures and river corridor, features are adjusted by manipulating the terrain model in GIS, upon which the computational domain is overlaid, and the floods simulated again. For each of these perturbations, mesh, boundary condition, and input parameters are identical; relief structures were deleted from the model geometry if a perturbation rendered them obsolete. Various output parameters can be used to assess results, including inundation extent and duration, backwater volume, velocity, water surface elevation, and peak flow arrival time and magnitude at structure locations and boundary conditions.

Two extremes are tested: existing conditions, and "natural" conditions, as defined by removal of all existing structures (bridges, culverts, rights-of-way, etc.) in the river corridor. Subsequently, the 14 bridges between Proctor Falls and Leicester Junction (Figure 4.1) were selected for detailed sensitivity analysis. These were chosen based on bridge density—in terms of number of structures per river mile—and for utility of results in terms of separating the impacts of structures from natural floodplain functions. The three structures above Proctor Falls were omitted because of the lack of hydraulic connectivity through the dam. Downstream of Leicester Junction, the floodplain nearly doubles in width, bridges are spatially sparse, and peak flows have already been attenuated by nearly 40%.

These 14 bridges and associated roadways/grades were removed individually to elucidate the impacts of each on the network. While of course wholesale removal of bridges and roadways is, in most cases, impractical, the presumption is that any infrastructure upgrades will be a step in the direction of establishing more natural conditions, either through a wider, pier-free span, or installation of relief structures (Johnson, 2002). In fact, these modifications, taken to potentially cost-prohibitive extremes, can result in flows that are virtually identical to natural conditions. This analysis identifies both the structures to which the network is most sensitive (governing structures) and the structures that are most sensitive to the network (sensitive structures). From here, more realistic perturbations are applied to the governing structures to determine more accurately the potential impacts of practical upgrades.
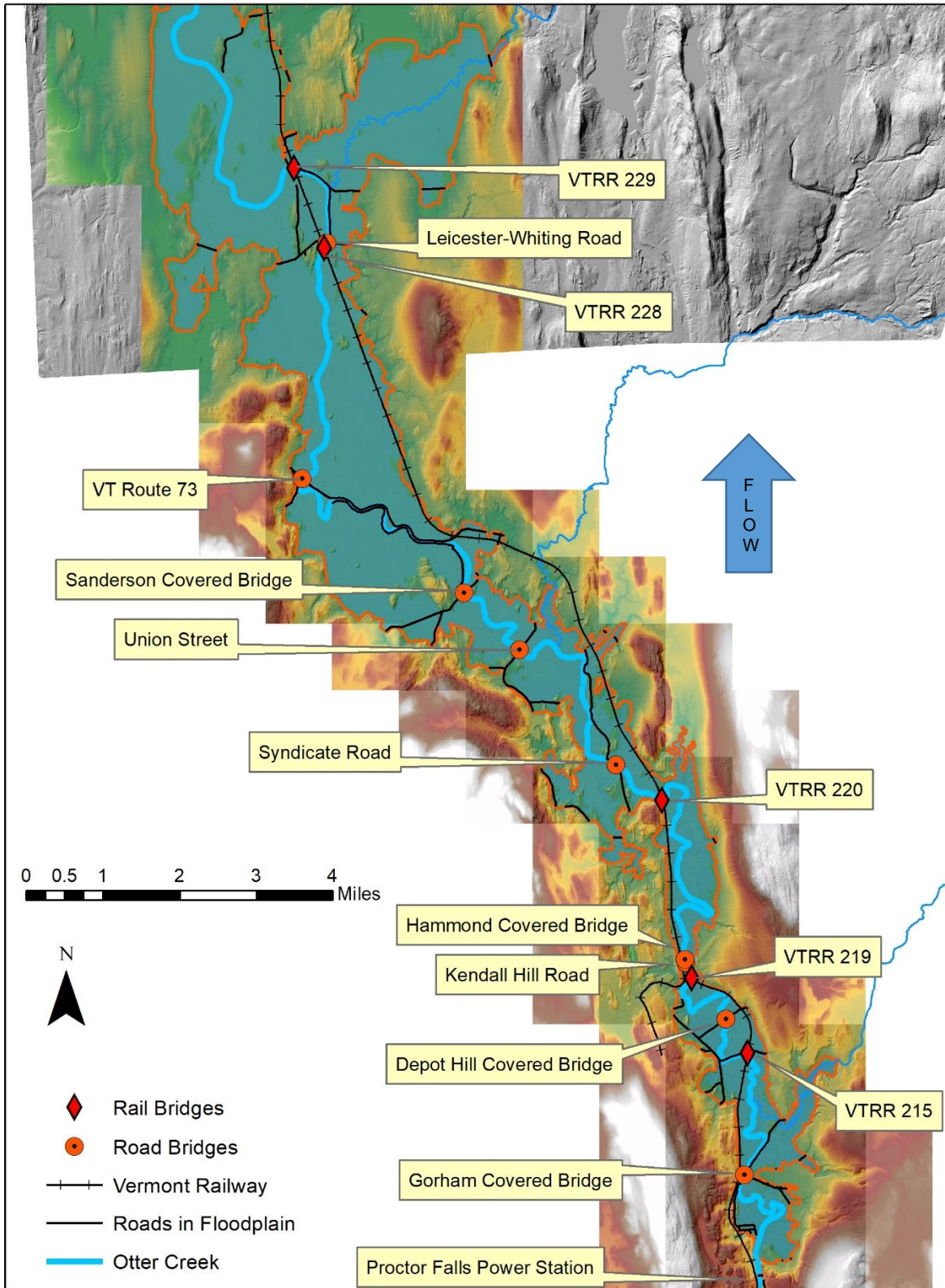
Figure 4.1: Locations of 14 bridges selected for analysis. Flow is south-to-north.

Additionally, certain combinations of perturbations are simulated, such as removal of the entire Vermont Railway Northern line, while leaving all highway bridges as-is. Further attention is also paid to the complex interactions at Florence and Leicester Junctions, where at both sites, the Otter Creek is spanned by three bridges within several hundred feet. These are natural geologic constrictions in the river's floodplain, a common location for bridge crossings on many rivers. However, natural constriction can be exacerbated by right-of-way and abutment encroachment, and repeated road/rail crossings effectively increase the length of the constriction; i.e., rather than a relatively short geological feature in terms of length of constricted flow, wherein high velocities may be immediately attenuated on the downstream floodplain, the successive bridge constrictions have the effect of forcing higher velocities through a much longer river reach.

4.2   Assessed Bridges

Existing structure data are tabulated below in downstream order. Bridges range in age from several years to over a century and represent a variety of designs and hydraulic characteristics (Table 4.1). With the exception of railroad structures and two highway bridges (Kendall Hill Road and VT Route 73), all bridge spans constrict the channel to some degree. Most are entirely inadequate for modeled floods, based on the criterion of the discharge that allows one foot of freeboard, measured one bridge-length upstream (VTrans, 2015), which is exceeded in nearly all cases, so much that low velocities and overtopping relief are paramount to their resiliency (Table 4.2). Modeled flows are substantially less than estimated values based on USGS Streamstats regressions at bridge locations (Olson, 2014), indicating that these predictions cannot be taken at face value for all locations and rivers (Table 4.3).

Based on assessed sensitivity to Q25, 50, 100, and TS Irene flows, perturbations are only tested for the five most impactful structures (VTR 215, 219, 220, Leicester-Whiting Rd., and VT Route 73) for Q500 flows.

Table 4.1: Physical characteristics and ratings of structures as of most recent inspection. Ratings are color-coded; green meaning more adequate, orange indicating deficiency. See Appendix for rating descriptions.

Road/Bridge	Route Name	Town	Overall Condition	Federal Sufficiency Rating	Scour Rating	Waterway Adequacy	Channel Rating	Superstructure	Substructure	Year Built/ Rebuilt	n spans	Total Span (ft)	Detour Length (mi)	Mean Daily Traffic
Gorham Bridge	C3006	Proctor	N/A	30	8	5	7	6	8	1841/ 2004	1	109	4	550
VTR 215	VTR Northern	Pittsford	6	N/A				6	6	1900	2	207	N/A	
Depot Hill Rd	C3023	Pittsford	N/A	61.6	3	7	6	5	5	1840/ 1985	1	108	3	700
VTR 219	VTR Northern	Pittsford	6	N/A				6	7	1900	2	210	N/A	
Kendall Hill Rd	FAS 0155	Pittsford	N/A	49.5	5	8	6	6	5	1960	4	276	6	1720
Hammond Bridge	N/A	Pittsford	Historic Structure, closed to vehicle traffic							1842/ 1928?	1	139	0	0
VTR 220	VTR Northern	Pittsford	4	N/A				6	4	1899	2	210	N/A	
Syndicate Rd/ Carver St	C3042	Brandon	N/A	51.8	8	6	6	6	6	1851/ 1929	1	109	8	30
Union St	C2005	Brandon	N/A	95.7	8	8	8	8	7	1992	1	130	7	500
Sanderson Bridge	C2004	Brandon	N/A	30.3	8	8	8	7	7	1838/ 2003	1	116	7	600
VT Route 73	VT73	Sudbury	N/A	85.9	8	3	6	7	6	1952	3	235	25	1900
VTR 228	VTR Northern	Leicester	6	N/A				6	5	1929	1	156	N/A	
Leicester-Whiting Rd	FAS 0160	Leicester	N/A	86.2	8	7	8	8	8	2006	1	110	18	1150
VTR 229	VTR Northern	Leicester	6	N/A				6	6	1896	1	157	N/A	

Table 4.2: Structure hydraulic characteristics.

Road/Bridge	Total Span (ft)	Bankfull Upstream (ft)	Bankfull Downstream (ft)	Maximum Safe Discharge (cfs) [1 ft freeboard , 1 bridge length upstream]	Q50 Peak Velocity (fps)	Roadway overtopping WSE (ft, NAVD88)	Bridge Low Chord (ft, NAVD88)	Peak WSE Q25 (ft, NAVD88)	Peak WSE Q50 (ft, NAVD88)	Peak WSE Q100 (ft, NAVD88)	Peak WSE Q500 (ft, NAVD88)	Peak WSE TS Irene (ft, NAVD88)
Gorham Bridge	109	128	143	6,160	4.9	360.25	362.55	365.77	366.49	367.44	368.72	367.67
VTR 215	207	141	142	9,540	4.9	361.40	363.37	364.49	365.31	366.39	367.77	366.52
Depot Hill Rd	108	121	112	4,530	2.1	356.15	359.93	364.39	365.24	366.32	367.73	366.45
VTR 219	210	135	128	16,250	4.8	365.18	363.86	363.90	364.75	365.83	367.24	365.96
Kendall Hill Rd	276	128	95	21,200	6.9	368.55	370.75	363.04	363.83	364.85	366.13	364.95
Hammond Bridge	139	95	151	9,800	5.5	362.65	362.22	362.91	363.67	364.62	365.83	364.68
VTR 220	210	115	110	10,000	5.8	362.22	360.58	360.81	361.53	362.39	363.47	362.42
Syndicate Rd/ Carver St	109	112	138	3,700	3.1	352.87	355.99	359.73	360.32	361.04	361.99	361.07
Union St	130	138	128	20,000	4.0	353.20	360.25	356.22	356.71	357.27	358.02	357.20
Sanderson Bridge	116	154	148	21,000	5.0	351.40	359.27	355.17	355.59	356.15	356.87	356.02
VT Route 73	235	108	115	10,300	3.8	349.69	352.05	352.81	353.30	353.89	354.71	353.63
VTR 228	156	115	125	7,850	4.5	351.40	352.05	350.84	351.20	351.69	352.48	351.40
Leicester-Whiting Rd	110	125	121	12,600	5.0	349.10	352.71	350.67	351.03	351.49	352.35	351.20
VTR 229	157	121	131	7,200	3.3	351.72	351.89	349.59	350.05	350.67	351.82	350.15

Table 4.3: Modeled peak flows at bridge locations; Streamstats values from Olson (2014).

Road/Bridge	Peak Discharge (cfs)								TS Irene
	Q25		Q50		Q100		Q500		
	Model	Streamstats	Model	Streamstats	Model	Streamstats	Model	Streamstats	Model
Gorham Bridge	12,070	20,700	13,720	24,500	15,400	28,400	18,240	39,300	17,620
VTR 215	12,320	22,800	14,098	26,900	16,660	31,200	20,405	43,200	17,660
Depot Hill Rd	12,480	22,900	14,098	27,100	16,460	31,400	19,953	43,400	17,370
VTR 219	12,280	23,000	13,896	27,200	16,240	31,500	19,692	43,500	17,050
Kendall Hill Rd	12,270	23,000	13,879	27,200	16,230	31,500	19,685	43,500	17,020
Hammond Bridge	12,270	23,000	13,879	27,200	16,230	31,500	19,681	43,500	17,020
VTR 220	11,570	23,100	13,268	27,300	16,230	31,700	18,876	43,700	15,840
Syndicate Rd/Carver St	11,440	23,000	13,120	27,200	15,220	31,600	18,166	43,500	15,480
Union St	11,230	24,200	12,971	28,500	15,300	33,100	18,657	45,500	15,290
Sanderson Bridge	11,020	24,200	12,731	28,500	15,020	33,100	18,350	45,500	15,000
VT Route 73	10,130	23,900	11,753	28,300	14,050	32,700	15,828	44,900	13,530
VTR 228	6,130	23,700	7,098	27,900	7,850	32,300	9,853	44,400	7,350
Leicester-Whiting Rd	8,590	23,700	10,842	27,900	12,590	32,300	16,457	44,400	11,440
VTR 229	5,260	24,200	6,145	28,500	7,180	32,900	6,145	45,000	6,620

4.3 Total Impacts

The combined effects of all structures between Rutland and Middlebury result in attenuation of peak flows in Middlebury by approximately 300 - 400 cfs in all modeled floods (Table 4.4). In synthetic events, this is in addition to roughly 5,000 cfs of peak attenuation provided by the valley's natural features (e.g., floodplains and natural constrictions). Note that in TS Irene, peak flows are reduced by over 9,000 cfs, a consequence of its flashier hydrograph, and that the amount of this attributable to structures is greater than the artificial floods, albeit more comparable. What this means for the Otter Valley is that the natural function of the existing floodplain is far more valuable than any flood control services provided by all encroaching infrastructure combined. Therefore, any proposed alterations to any single bridge are unlikely to dramatically affect the overall flood response of the Otter Creek as a whole. However, the acute impacts of such perturbations can change flow conditions at other structures and propagate miles up- and downstream. The network is more sensitive to certain structures, and certain structures are more sensitive to the network.

Table 4.4: Flow attenuation provided by natural features and structures.

Flood Event	Rutland Peak (cfs)	Middlebury Peak – Existing (cfs)	Middlebury Peak – Natural Conditions (cfs)	Total Attenuation by Structures (cfs)
Q-25	10,500	5,010	5,440	430
Q-50	11,700	6,130	6,550	420
Q-100	12,900	7,590	7,950	360
Q-500	15,600	10,460	10,720	260
TS Irene	15,700	6,075	6,540	465

4.4 Impacts to Network

The impacts of local adjustments to structures in the network can be assessed by changes in peak discharge, measured at each crossing location. A perturbation-induced change in discharge throughout the network does not necessarily correspond with other bridges' sensitivity thereto. These network impacts represent the potential for sensitivity, contingent upon characteristics that dictate the response of affected bridges, discussed in the next section.

Adjustments at any structure can result in changes in discharge and WSE that propagate throughout the entire model domain. These can be significant, minor, or inconsequential, largely dependent on the magnitude of the imposition of the existing structure on the floodplain. Vermont Railway Bridges 215, 219, and 220 have the most profound impact on the network in terms of both magnitude and spatial extent (Table 4.6). The network is insensitive to structures that do not substantially alter natural conditions at their

locations, and adjustments to these bridges do little to impact surrounding bridges (e.g., Depot Hill Rd., Figure 4.2). Structures that dramatically affect local flow dynamics will also govern conditions at downstream structures (e.g., VTR 220, Figure 4.3).

Combinations of a bridge and right-of-way that excessively constrict flow paths will result in substantial backwaters (Table 4.5). Note that while the bridge span itself may impose a lateral constriction, the associated roadway creates a vertical constriction, like a weir. For a river with considerable floodplain access like the Otter Creek, the latter may be more significant than the former. The bridges to which the network is most sensitive are railroad bridges with elevated grades that traverse the floodplain. However, these bridges are among the most impressive spans over the Otter Creek, nearly doubling the length of most others, but the additional span length does not restore the conveyance eliminated by over a mile of an 8-12 foot-high embankment. Compare this with an inadequate structure in terms of channel constriction, but a road that is barely elevated off the floodplain (e.g., Depot Hill Rd., Syndicate Rd.). When the river spills its banks, overbank flow is essentially unrestricted, and the constriction of the bridge loses significance because of the massive additional available conveyance. When flow is confined to the channel, at or below bankfull discharge, the geometry of the bridge is a very important consideration for that structure's stability. However, once sufficient floodplain activation has occurred, as it does in all modeled floods, the roadway geometry becomes far more significant in governing the conditions at the bridge, and its impact on the network. Note that the three shortest-spanned bridges (Gorham, Depot, Syndicate) are also the least consequential to the network in modeled floods, and that the three longest-spanned bridges (VTR 215, 219, 220) have the greatest impact (Table 4.6).

Adjustments to the structures that create the largest backwaters result in the greatest impacts to the network. An increase in storage will attenuate discharge, and a reduction in backwater storage will result in an increase in downstream peak flows, which can be accomplished by an increased span or provision of additional relief. This is a simple mass-balance, and applies generally under steady-state conditions. However, the intricacies of transient flow can complicate this relationship, leading to interesting, counter-intuitive situations.

Table 4.5: Right-of-way physical characteristics and relation to peak backwater storage and proportion of flood wave (excluding base flow) that pass through each structure. In general, backwater volumes will dictate network sensitivity, while proportion of flow through a bridge will determine structure sensitivity.

Bridge	Min Grade Elevation above Floodplain (ft)	Road Length in Floodplain (ft)	Peak Backwater Storage Volume (acre-feet)					Percent of Flood Flow through Bridge Span(s) (Including Relief Structures/Culverts)				
			Q25	Q50	Q100	Q500	TS Irene	Q25	Q50	Q100	Q500	TS Irene
Gorham	1.3	1,109	18.7	13.9	15.6		15.9	81.5%	80.8%	79.3%	75.5%	69.2%
VTR 215	7.7	6,037	274.9	237.9	208.6	190.4	208.6	79.0%	72.5%	66.1%	59.9%	53.9%
Depot	1.0	3,609	57.1	54.6	60.6		58.1	30.5%	31.4%	30.2%	27.1%	23.4%
VTR 219	10.8	1,723	243.1	280.8	376.1	471.5	393.3	100%	100%	99.9%	99.0%	99.7%
Kendall	12.2	463	56.5	69.4	88.4		91.2	100%	100%	100%	100%	100%
Hammond	6.3	427	56.0	66.3	80.0		81.7	99.9%	99.8%	95.6%	98.8%	99.1%
VTR 220	12.8	1,312	215.5	240.0	344.6	399.2	313.6	100%	100%	99.9%	99.1%	99.9%
Syndicate	1.6	2,165	81.4	87.2	90.8		92.9	44.9%	45.6%	45.2%	39.4%	34.7%
Union	1.8	2,854	106.7	101.0	119.0		114.7	61.7%	61.3%	59.2%	55.1%	51.8%
Sanderson	1.6	4,429	257.7	240.6	249.2		254.3	79.3%	77.4%	75.2%	70.5%	70.3%
Route 73	1.9	12,668	267.4	217.6	188.7	161.1	185.1	44.3%	43.2%	41.0%	36.6%	31.8%
VTR 228	5.6	5,676	309.4	335.6	365.0		340.5	99.9%	99.6%	97.4%	91.0%	98.7%
Leicester-Whiting	3.3	4,889	701.7	844.4	691.1	549.3	725.7	76.4%	73.2%	70.8%	62.7%	67.3%
VTR 229	5.9	4,331	645.8	671.4	658.8		788.4	94.0%	91.2%	88.3%	84.7%	89.5%

The presence of a constricting, backwater-inducing structure can actually increase peak flows downstream in certain conditions. Specifically, if that bridge, after detaining a large volume of water, experiences substantial and simultaneous relief as the flood peak crests, a surge in the flood wave will then propagate downstream, leading to greater peak discharges than if the structure were removed. This phenomenon was observed at one railroad crossing (VTR 215), which caused some of the most substantial changes to downstream discharge magnitude (Figure 4.8). To a lesser degree, the Vermont Route 73 highway crossing also exhibits this behavior. These structures are prime candidates for rehabilitation, as interventions to improve local hydraulics will benefit the network as well, reducing both downstream peak flows and backwater inundation.

In all other cases, improving conveyance at a backwater-inducing structure results in increased peak discharge downstream, and may or may not impose additional hazard on other infrastructure, depending on the characteristics of the affected locations in the network.

Upstream impacts can also occur due to these interventions. The Otter Valley is shallow enough, and backwaters substantial enough, that many of the larger structures impose tailwater controls on upstream bridges. These then create greater backwaters, and the effect cascades upstream. Thus these governing structures can affect discharge upstream in addition to downstream.

Table 4.6: Impact matrix of individually removed structures for Q100. Positive values (orange) indicate an increase in discharge (cfs) following structure removal; negative values (green) indicate a decrease. Read horizontally for impact of a bridge on the network. Diagonal entries indicate effects at perturbed bridge site. Results for Q25, 50, 500, and TS Irene are tabulated in Appendix.

Δ Peak Discharge Q100 (cfs)		Impact on Bridge													
		Gorham	RR 215	Depot	RR 219	Kendall	Hammond	RR 220	Syndicate	Union	Sanderson	Rt 73	RR 228	LW	RR 229
Existing		15,400	16,660	16,460	16,240	16,230	16,230	16,230	15,220	15,300	15,020	14,050	7,850	12,590	7,180
Removed Bridge	Gorham	-2.9	17.9	22.5	24.7	26.1	24.8	17.2	15.1	16.7	15.9	10.8	4.8	8.2	2.5
	RR 215	-27.2	190.8	-123.1	-110.2	-107.5	-108.6	-87.9	-77.2	-74.8	-71.8	-40.9	-17.4	-22.9	-1.6
	Depot	7.4	12.4	32.9	17.7	19.0	17.7	10.2	9.0	9.7	9.1	4.2	0.9	1.2	-0.1
	RR 219	54.0	151.2	199.8	180.7	181.4	180.2	135.1	118.6	125.4	121.8	77.3	32.9	50.4	12.5
	Kendall	12.6	34.0	43.7	45.4	46.6	45.2	33.5	29.3	30.6	29.1	18.7	8.1	13.2	3.3
	Hammond	10.6	26.4	31.6	32.6	34.0	38.0	23.9	21.4	23.3	22.2	15.2	6.9	10.6	3.5
	RR 220	20.7	60.6	100.8	126.1	128.9	127.8	173.8	152.3	158.5	153.9	105.2	43.9	69.2	18.1
	Syndicate	8.9	21.7	27.7	30.2	31.6	30.3	16.8	54.8	15.8	15.1	14.1	6.7	12.6	4.8
	Union	8.2	19.6	24.6	26.7	28.1	26.8	16.4	19.1	10.5	4.8	-1.4	-3.7	-5.7	-2.4
	Sanderson	8.0	19.9	26.1	29.7	31.1	29.8	28.6	34.9	22.6	162.8	3.0	3.4	11.4	7.2
	Rt 73	7.8	18.5	23.2	25.3	26.7	25.4	17.0	18.0	13.0	3.4	-952.9	-48.8	-78.6	-27.9
	RR 228	7.7	19.0	23.9	26.1	27.5	26.2	18.3	16.1	18.4	20.0	90.8	805.9	27.8	354.9
	LW	7.7	19.0	23.9	26.1	27.4	26.2	18.3	16.1	22.7	33.6	108.1	-767.0	478.2	-657.1
	RR 229	7.7	19.1	23.8	26.1	27.4	26.2	18.3	16.0	17.6	16.9	0.9	245.0	125.8	366.9

Figure 4.2: Comparison of Q100 discharge at Depot Hill Rd under existing (left) and natural conditions (right). Subtle differences exist in the proportion of channel versus overbank flow, but total discharge remains essentially the same, and the effect is inconsequential to the network (Table 4.6).
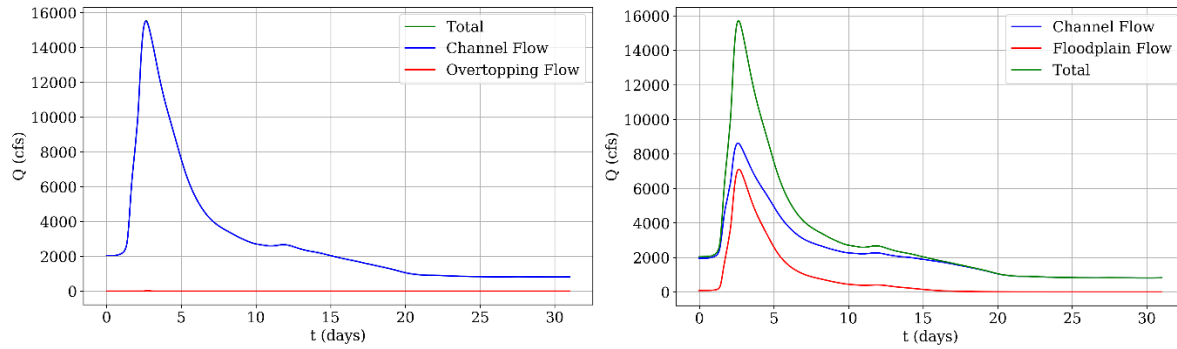
Figure 4.3: Comparison of Q100 discharge at Vermont Railway Bridge 220 under existing (left) and natural conditions (right). The entirety of flow is through the structure as it is; removal allows floodplain flow and eliminates the backwater created by the structure, resulting in a slightly sharper total hydrograph peak and increased peak flows downstream (Table 4.6).

Network sensitivity to Rail Bridges 228, 229, and Leicester-Whiting Road is also considerable, albeit far more localized and for more complex reasons. Leicester-Whiting (L-W) Road creates the largest backwater of all structures on the Otter Creek, but not because of the bridge that spans it. West of its river crossing, L-W Road traverses a low-lying wetland, which is perforated by a modest 20' span × 6' rise box culvert (Figure 4.4). In flood stage, this is actually the river's preferential flow path, but the undersized culvert cannot convey all requisite floodplain flow (Figure 4.5). The resulting bottleneck forces unnaturally high flow through the river channel and VTR Bridges 228 and 229, and the main span of L-W Road. In all modeled floods, the road ultimately overtops both at the western culvert and adjacent to the main span under existing conditions. Replacement of this road and culvert with a clear span can reduce peak flows through the three main structures by 600 - 800 cfs, making this the most dramatic intervention tested in terms of magnitude, if not number of affected structures. This would also reduce backwaters to the point that L-W Road and the railroad would no longer overtop in floods less than Q100, allowing them to remain passable.
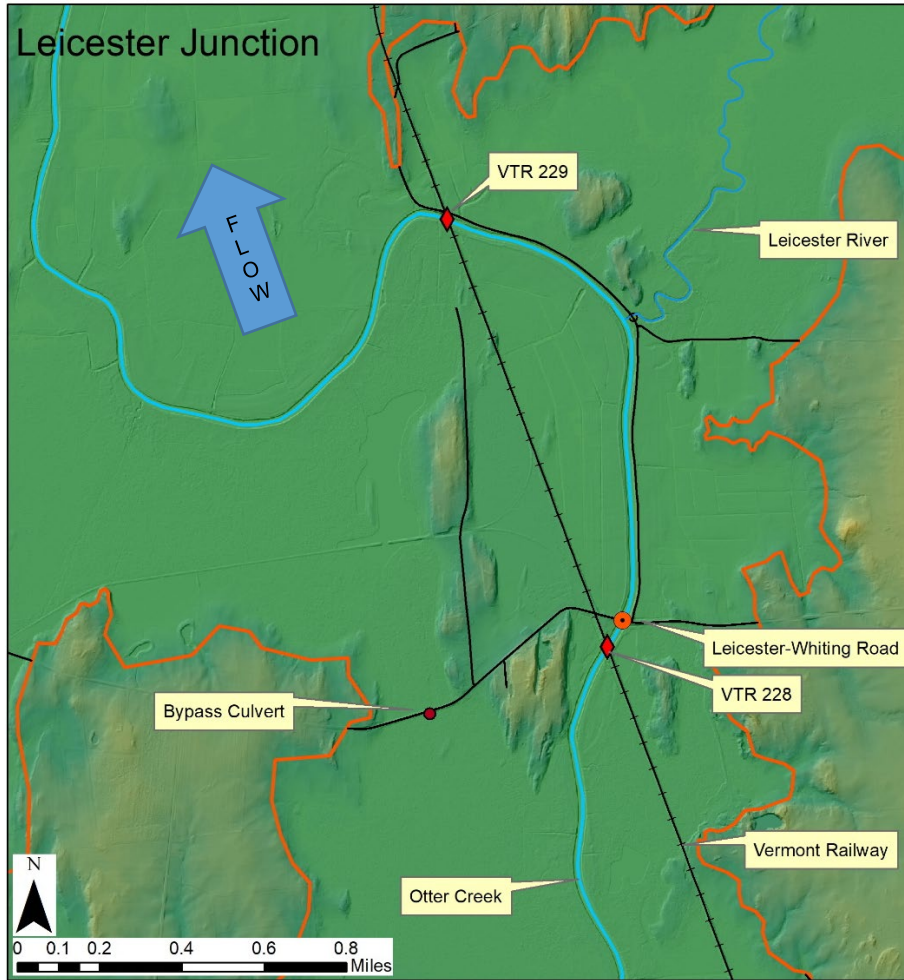
Figure 4.4: Leicester Junction. Flow is south-to-north. The road grade west of the main channel reduces flows that would otherwise bypass VTR 228, 229, and the L-W Road bridge. Replacement of this road and culvert with a clear span reduces flows through these bridges by 600-800 cfs and eliminates as much as 700 acre-ft of backwater inundation. The rail grade creates substantial backwaters in the Leicester River as well.

Similarly, impacts of perturbations at Florence Junction are difficult to untangle. This is the most pronounced natural constriction in the study area (that does not create a waterfall), so to some degree, backwaters and flow attenuation will occur regardless of the three bridges that span Otter Creek here. The Kendall and Hammond Bridges cross the river more or less at the floodplain's narrowest point. These are sensitive for that reason as discussed in the next section, but because of this and the fact that they are less than 200 feet apart, adjustments to one will pass the hydraulic control onto the other. VTR 219 is somewhat different because it establishes the constriction several hundred feet upstream and leads to higher velocities in the intermediate channel (Figure 4.6). Removal of individual structures, especially VTR 219, will substantially reduce proximal channel velocities, though peak velocities through the unperturbed structures

are less affected. The higher velocities maintained for a longer reach of river due to these three bridges may have high geomorphic significance.

At VT Railway Bridge 215, which causes peak flow magnification under existing conditions, two relief structures are present in the adjacent floodplain—VTR Bridges 214 and 217. These have 16' and 12' spans, respectively, and convey peak flows between 700 - 1,100 cfs and 500 - 900 cfs for modeled floods; overtopping flows then exceed 5,000 - 14,000 cfs. Overbank flows without the bridges and rail grade consistently surpass 10,000 cfs. These are the most substantial relief structures in the study area, and are inadequate for all modeled floods, though they may be sufficient for more frequent events (e.g., $\leq$ Q10). In this case, where overtopping may not occur, network sensitivity to this structure would likely be comparable to that of VTR 219 or 220, which attenuate peak flows rather than intensifying them.
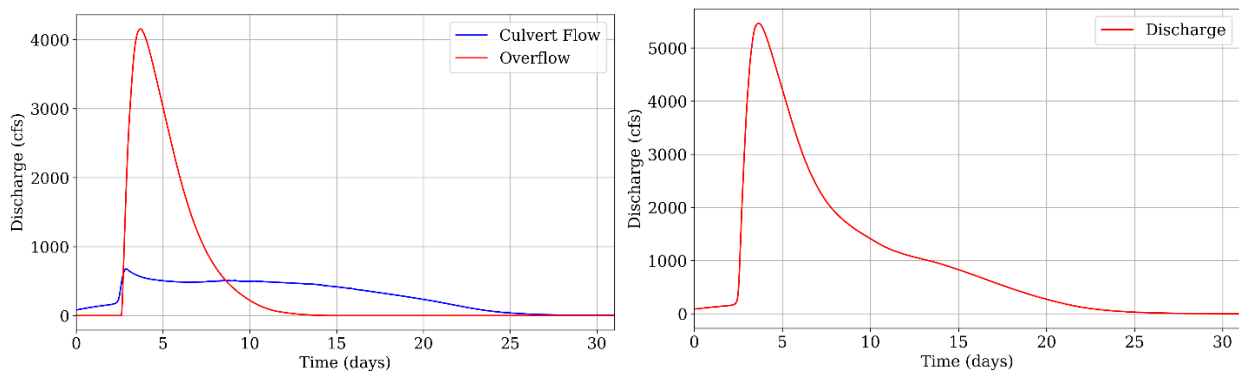
Figure 4.5: (Left) Bypass culvert discharge on L-W Rd, west of its main Otter Creek crossing, in synthetic Q100 flood; (Right) Flow through artificial clear span replacement.

The magnitude of the flood will affect network sensitivity to a given perturbation (Table 4.4). This is largely dependent on roadway overtopping elevations in relation to peak WSE. For example, changes in discharge due to removal of Leicester-Whiting Road are maximized in the Q50 flood, while Rail Bridge 219 has its greatest impact in Q500.

4.5   Impacts to Structures

The network impacts discussed above may or may not significantly change conditions at individual structures. Generally speaking, this depends on the proportion of flood flows that pass through a bridge's span rather than via relief (Table 4.5). While overtopping flows can damage road surfaces and embankments, repairs are often rapid and inexpensive compared to a damaged or failed bridge. Because of this, changes in peak channel velocity, through the bridges, are used as a proxy to determine how sensitive individual structures are to the assessed perturbations on the network. Channel velocities can be related to

site-specific hazards like scour, and are important considerations for VTrans' design of structures and sizing of countermeasures (VTrans, 2015).
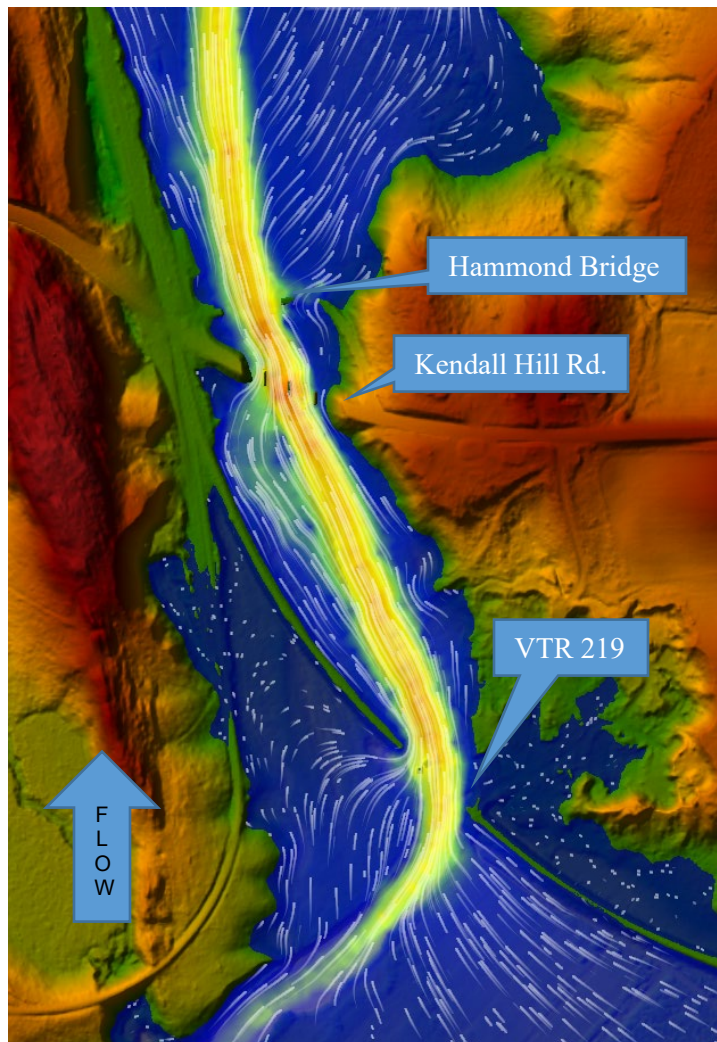
Figure 4.6: Peak velocity (6-8 fps) and flow paths through VTR Bridge 219, Kendall Hill Rd., and Hammond Covered Bridge in TS Irene. Image is 0.35 miles across. The natural constriction imposed by the terrain is artificially established several hundred feet upstream by the railroad crossing. These three structures may be more sensitive to network perturbations because nearly all flow passes through their spans, and the peak velocity is associated with peak discharge (Case 1).

Modeled peak channel velocity for a flood event may occur either (1) contemporaneously with peak discharge (Case 1), or (2) at some lower total flow associated with the structure's maximum hydraulic impact (Case 2). In Case 1, the impacts of changes in peak discharge associated with perturbations elsewhere in the network have the maximum potential to affect that structure. Whether or not this manifests depends on the specifics of the crossing and the magnitude of change in discharge (ΔQ). If all or nearly all flow is in the channel and passes through the bridge, any increase in peak discharge will result in the maximum increase in velocity at the bridge (Figure 4.6). If, on the other hand, the right-of-way is only a

minor impediment to overbank flow, most flood flow is not through the span, any increases in velocity are distributed across a vast cross-section, and changes in hazard at the bridge itself will be minimal (Figure 4.7).
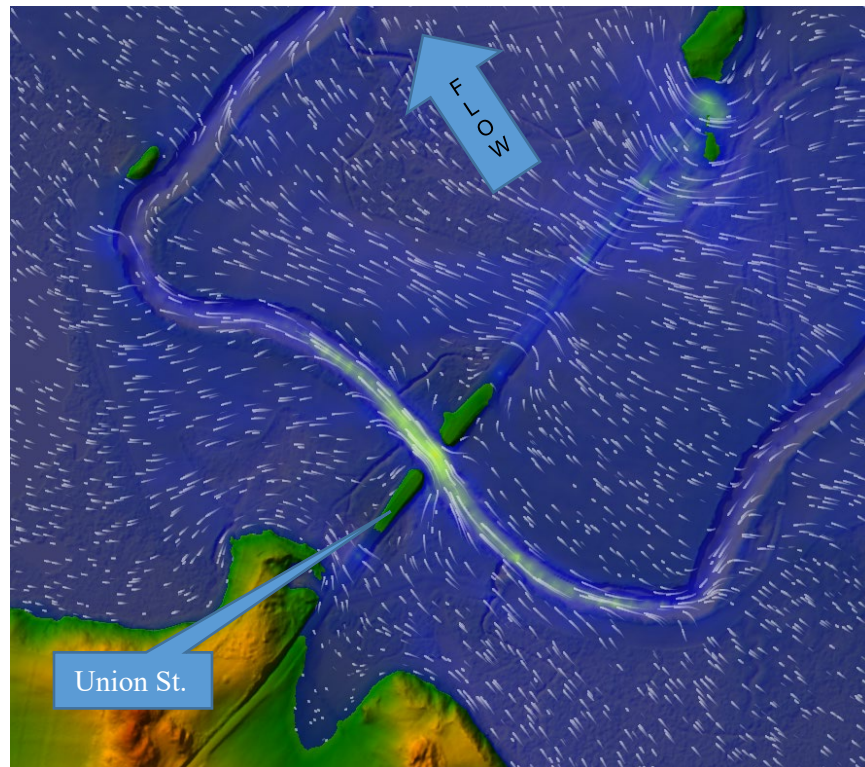
Figure 4.7: Peak velocity (3 fps) and flow paths through Union St. Bridge in TS Irene. Image is 0.6 miles across. Here, peak velocity is associated with peak discharge (Case 1), but substantial overtopping relief in the floodplain alleviates channel velocities significantly, and this structure is less sensitive to network perturbations.

For Case 2, peak velocity through the bridge occurs at the moment of impending relief (Figure 4.9). At this time, the maximum discharge achievable through the bridge is realized for a given hydrograph. Once the grade overtops and flows are no longer entirely concentrated through the span, discharge and velocity therein will reduce, even as the total discharge continues to rise. Another lesser peak is experienced on the falling limb of the hydrograph, as relief ceases (Figure 4.8). In these situations, the bridge is less sensitive to network perturbations because peak velocities occur at a discharge magnitude that is experienced regardless of the peak value. Given a threshold peak discharge, peak velocities for a given storm event are controlled by the hydraulics of the structure, not the network. If peak discharge is increased to the point that greater velocities than these occur with peak discharge, it becomes Case 1.
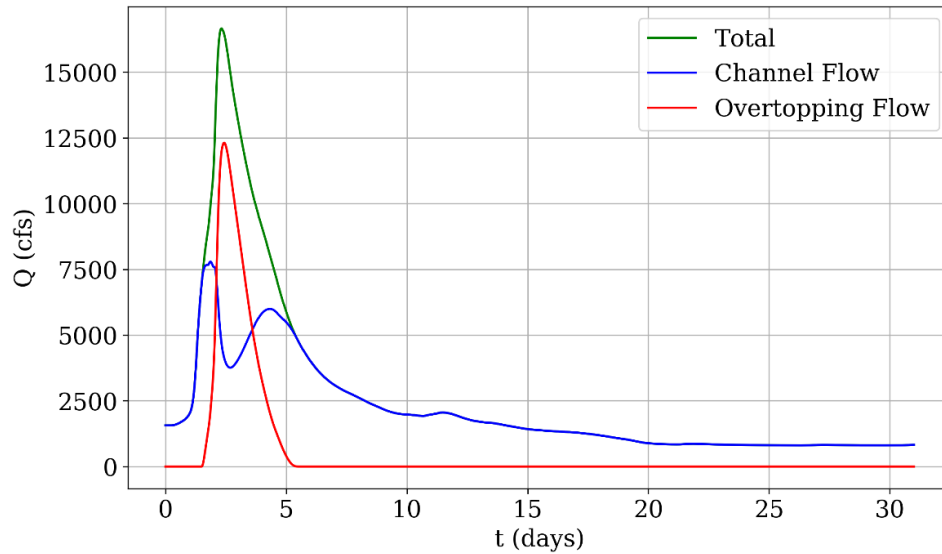
Figure 4.8: Hydrographs at Vermont Railway Bridge 215 in Q100 flood. Peak discharge through the structure occurs before the total peak arrives. The greatest velocities through this structure occur at this point. Subsequent overflow results in propagation of a surge in the flood wave downstream.
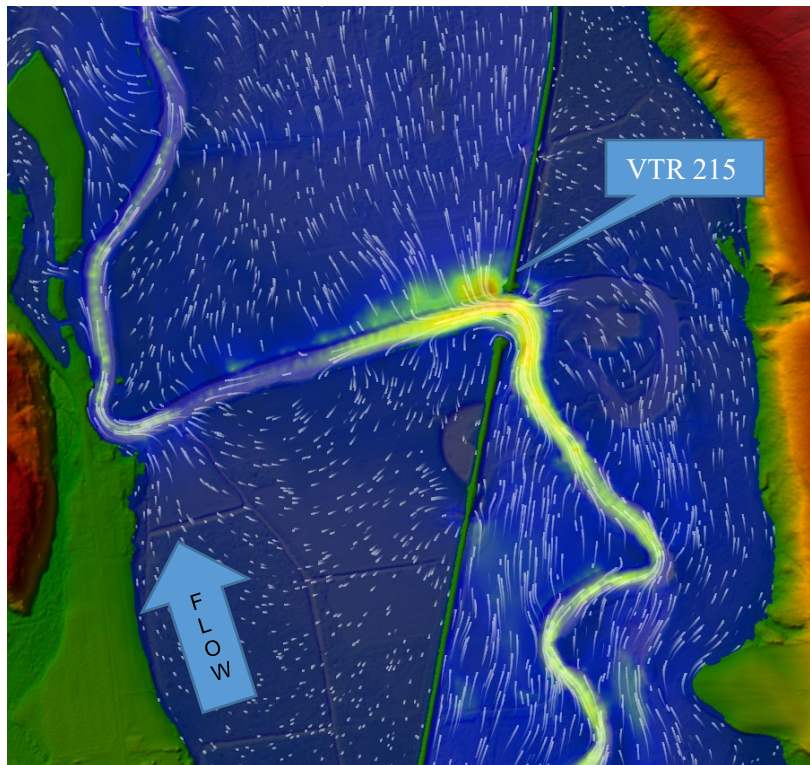
Figure 4.9: Velocity and flow paths through VTR 215 just before overtopping relief occurs in TS Irene. Image is 0.75 miles across. At this time, differences in WSE on the up- and downstream sides of the embankment exceed 3 feet, and peak velocity through the span is over 8 fps. When the flood wave reaches maximum discharge, 15 hours later, and overtopping flow has taken over (Figure 4.8), channel velocity is under 2 fps. This governing structure poses a hazard to itself, but is less sensitive to network perturbations because peak velocities occur independently of peak discharge (Case 2).

It is important to note that these classifications must be made on a case-by-case basis, vis-à-vis flood magnitude. A bridge may experience case (1) in a 100-year flood, but case (2) in a 25-year event. Likewise, a given perturbation may induce this potentially high-sensitivity change, though this was not observed.

Table 4.7: Impact matrix showing changes in velocity (fps) through structures following individual structure removals for Q100. Negative values (green) indicate reduction in velocity following perturbation; positive values (orange) indicate an increase. Read vertically for sensitivity of structure to network perturbations. Diagonal entries indicate effects at perturbed bridge site. Results for Q25, 50, 500, and TS Irene are tabulated in Appendix.

Δ Peak Velocity Q100 (fps)		Impact on Bridge													
		Gorham	RR 215	Depot	RR 219	Kendall	Hammond	RR 220	Syndicate	Union	Sanderson	Rt 73	RR 228	LW	RR 229
Existing		4.994	4.836	1.857	5.191	7.458	6.073	6.464	2.697	4.198	5.296	3.710	4.779	5.337	3.579
Removed Bridge	Gorham	-0.758	-0.003	0.005	-0.002	0.001	0.006	-0.001	0.003	0.001	0.003	-0.002	0.001	0.002	0.002
	RR 215	0.223	-2.689	-0.019	-0.031	-0.045	-0.033	-0.030	-0.001	-0.012	-0.013	-0.006	-0.012	-0.017	-0.001
	Depot	0.013	0.025	-0.269	-0.003	-0.001	0.004	-0.003	0.004	0.000	0.003	-0.002	-0.001	0.000	0.001
	RR 219	0.019	0.069	0.031	-0.602	0.028	0.052	0.031	0.007	0.015	0.022	0.000	0.014	0.021	0.006
	Kendall	-0.001	0.000	0.006	0.017	-0.584	-0.023	0.003	0.003	0.003	0.006	-0.002	0.002	0.004	0.002
	Hammond	0.000	0.004	0.007	0.010	0.015	-0.690	0.000	0.004	0.002	0.005	-0.002	0.001	0.003	0.002
	RR 220	-0.001	0.000	0.006	0.053	0.094	0.087	-2.246	-0.099	0.018	0.025	-0.001	0.017	0.026	0.008
	Syndicate	0.005	-0.001	0.008	0.004	0.010	0.013	0.010	-0.146	0.000	0.002	-0.005	0.000	0.001	0.002
	Union	0.005	0.000	0.011	0.001	0.005	0.009	0.004	0.103	-1.325	0.003	-0.015	-0.004	-0.005	0.000
	Sanderson	0.004	-0.001	0.007	0.000	0.003	0.008	0.009	0.034	0.129	-1.049	0.003	-0.004	-0.005	0.002
	Rt 73	0.005	0.001	0.012	-0.001	0.003	0.007	0.002	0.104	0.042	0.123	-2.086	-0.028	-0.037	-0.009
	RR 228	0.004	-0.002	0.005	-0.002	0.001	0.006	-0.001	0.003	0.001	0.004	0.001	-1.560	0.014	0.125
	LW	0.004	-0.002	0.005	-0.002	0.001	0.006	-0.001	0.004	0.002	0.008	0.024	-0.278	-1.785	-0.282
	RR 229	0.004	-0.002	0.005	-0.002	0.001	0.006	-0.001	0.004	0.001	0.004	0.008	-0.016	0.111	-1.385

Elimination of tailwater controls can result in some of the greatest increases in channel velocities at upstream structures, although this phenomenon is largely independent of the affected bridges' features. Certain bridge characteristics may contribute to the structure's sensitivity to changes in discharge regardless of tailwater controls; structures through which all flow passes may be most sensitive to increases or decreases in discharge.

Natural flow constriction may result in sensitivity of structures that otherwise fit the criteria of network insensitivity due to their physical characteristics alone. Syndicate Road, to which the network is insensitive, is barely elevated and experiences significant overtopping relief. However, terrain constrictions in its proximity reduce the available floodplain conveyance compared to up- and downstream, so this structure can be sensitive to perturbations, despite its ostensibly insensitive characteristics (Table 4.7).

Certain structures will be more sensitive if pressure flow is experienced through the span. This is most concerning at the historic Hammond Covered Bridge, which does not experience any relief until WSE exceeds the bridge's low chord elevation by more than 2 ft, and even then it is minimal. In fact, this structure was lifted from its abutments and carried more than a mile downstream by floodwaters in 1927. Excepting Rail Bridges 219 and 220, all other bridges either do not experience pressure flow under modeled floods,

or WSE reaches their low chord only after substantial overtopping relief has occurred, mitigating the additional hazard to a large degree. These impacts were not assessed because no perturbations resulted in changing whether or not other bridges experienced pressure flow, which is a complex, site-specific phenomenon that requires scour or sediment transport calculations to properly assess. Further, estimated model WSE errors of up to one foot or possibly more complicate this analysis. The risk of debris jams is high at many bridges on Otter Creek, which is reflected in inspection reports.

4.6   Discussion

Overall, the relative magnitude of impacts is, at most, on the order of 1-2% for both induced changes in discharge and resultant changes in channel velocity (Table 4.8). Because cross-sectional flow areas increase nonlinearly with increasing WSE, a considerable increase in discharge magnitude is required to effect an appreciable increase in velocity. This is good news for stable structures in good condition. However, even small changes may be enough to destabilize bridges that are structurally or hydraulically deficient. These would require a more detailed assessment based on estimated impacts of network perturbations.

Table 4.8: Percent changes in discharge due to perturbations in Q100. Governing structures generally induce changes between 1-2%. Note that the Leicester-Whiting Road crossing is somewhat unique (Figure 4.4).

Δ Peak Discharge Q100 (%)		Impact on Bridge													
		Gorham	RR 215	Depot	RR 219	Kendall	Hammond	RR 220	Syndicate	Union	Sanderson	Rt 73	RR 228	LW	RR 229
Removed Bridge	Gorham	-0.02%	0.11%	0.14%	0.15%	0.16%	0.15%	0.11%	0.10%	0.11%	0.11%	0.08%	0.06%	0.06%	0.03%
	RR 215	-0.18%	1.15%	-0.75%	-0.68%	-0.66%	-0.67%	-0.54%	-0.51%	-0.49%	-0.48%	-0.29%	-0.22%	-0.18%	-0.02%
	Depot	0.05%	0.07%	0.20%	0.11%	0.12%	0.11%	0.06%	0.06%	0.06%	0.06%	0.03%	0.01%	0.01%	0.00%
	RR 219	0.35%	0.91%	1.21%	1.11%	1.12%	1.11%	0.83%	0.78%	0.82%	0.81%	0.55%	0.42%	0.40%	0.17%
	Kendall	0.08%	0.20%	0.27%	0.28%	0.29%	0.28%	0.21%	0.19%	0.20%	0.19%	0.13%	0.10%	0.10%	0.05%
	Hammond	0.07%	0.16%	0.19%	0.20%	0.21%	0.23%	0.15%	0.14%	0.15%	0.15%	0.11%	0.09%	0.08%	0.05%
	RR 220	0.13%	0.36%	0.61%	0.78%	0.79%	0.79%	1.07%	1.00%	1.04%	1.02%	0.75%	0.56%	0.55%	0.25%
	Syndicate	0.06%	0.13%	0.17%	0.19%	0.19%	0.19%	0.10%	0.36%	0.10%	0.10%	0.10%	0.09%	0.10%	0.07%
	Union	0.05%	0.12%	0.15%	0.16%	0.17%	0.17%	0.10%	0.13%	0.07%	0.03%	-0.01%	-0.05%	-0.04%	-0.03%
	Sanderson	0.05%	0.12%	0.16%	0.18%	0.19%	0.18%	0.18%	0.23%	0.15%	1.08%	0.02%	0.04%	0.09%	0.10%
	Rt 73	0.05%	0.11%	0.14%	0.16%	0.16%	0.16%	0.10%	0.12%	0.08%	0.02%	-6.78%	-0.62%	-0.62%	-0.39%
	RR 228	0.05%	0.11%	0.15%	0.16%	0.17%	0.16%	0.11%	0.11%	0.12%	0.13%	0.65%	10.27%	0.22%	4.94%
	LW	0.05%	0.11%	0.15%	0.16%	0.17%	0.16%	0.11%	0.11%	0.15%	0.22%	0.77%	-9.77%	3.80%	-9.15%
	RR 229	0.05%	0.11%	0.14%	0.16%	0.17%	0.16%	0.11%	0.11%	0.12%	0.11%	0.01%	3.12%	1.00%	5.11%

All else being equal, this system-based analysis can prioritize structures for rehabilitation or replacement based on network impacts or sensitivity thereto. For example, if multiple structures are under consideration, a more sensitive structure should be temporally prioritized over a governing structure, avoiding the situation where replacement of the latter destabilizes the former. This must be weighed against timely mitigation of local hydraulic issues—scour-critical bridges must be addressed before failure occurs, even if this is not the most cost-effective solution in the long term. Additionally, this analysis can present novel techniques for improving a structure's resiliency without directly altering it. For example, covered

bridges are unlikely to be appreciably modified due to their historic and aesthetic value, but backwater-inducing structures upstream may act as effective countermeasures to reduce peak flows at the historic bridge—assuming stability of the governing structure. Whether or not this is sufficient must be assessed case-by-case.

Rating curves (stage-discharge relationships) may also be used to predict a structure's network impacts. The relation of roadway overtopping elevation to the inflection point of the rating curve may indicate the magnitude of influence the structure has on flow dynamics. Under natural conditions, the curve will rise steeply while flows are confined to the channel, inflect at bankfull discharge, and flatten as floodplain flow takes over. Insensitive structures may be identified by their lack of influence over the rating curve (Figure 4.10). A governing structure may shift or otherwise alter the natural inflection, and require a greater WSE for a given discharge beyond bankfull (Figure 4.11).
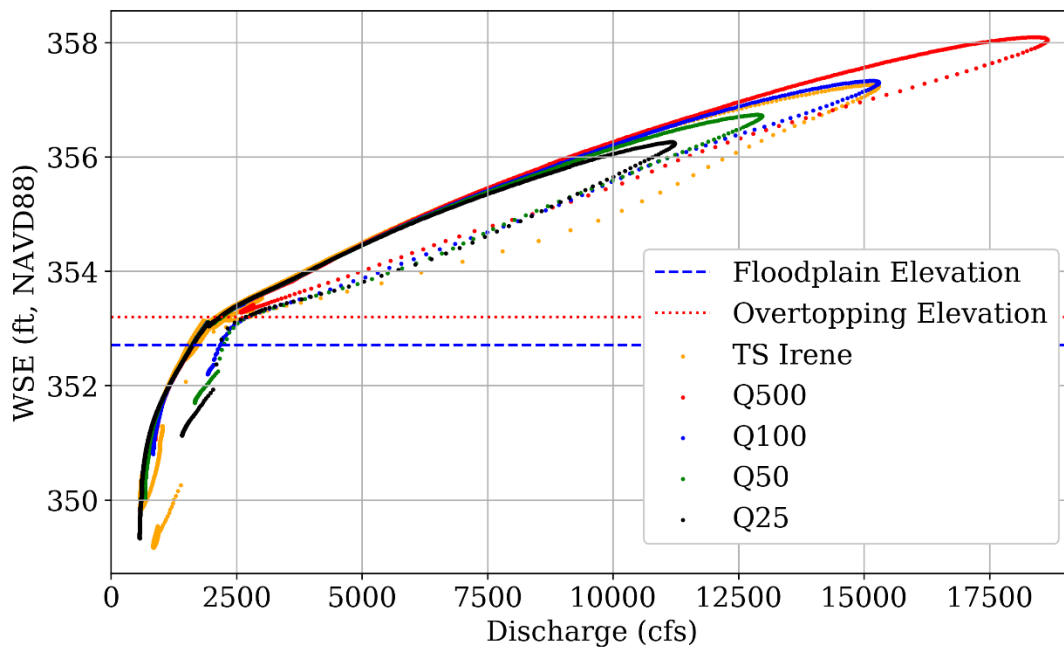
Figure 4.10: Rating curve at Union Street crossing. Roadway overtopping is initiated at the inflection point of the stage-discharge relationship. This permits fairly natural floodplain flow, and the network is insensitive to this structure.
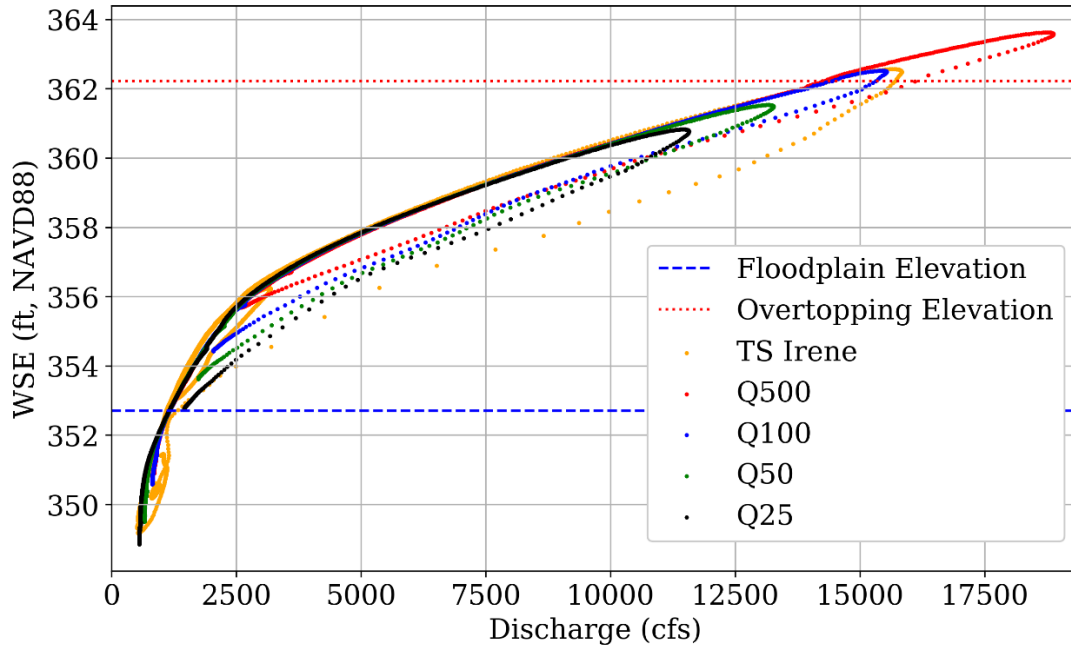
Figure 4.11: Rating curve at VTR 220 crossing. Inflection is smoothed due to inactivation of floodplain flow, and grade elevation is not exceeded until maximum discharges are realized. The network is highly sensitive to this structure.

The simple flow-chart presented in Figure 4.12 provides a decision tree for identifying sensitive and governing structures, and is applicable to all 14 assessed bridges on the Otter Creek under all modeled flow conditions. This is the result of distillation of impact matrices (e.g., Table 4.6, Table 4.7), backwater/relief assessment (Table 4.5), and analysis of the temporal distribution of peak velocities. This may assist in decision-making as to whether or not a network-scale analysis is necessary for a proposed alteration, or if modeling efforts ought to encompass nearby structures as well.
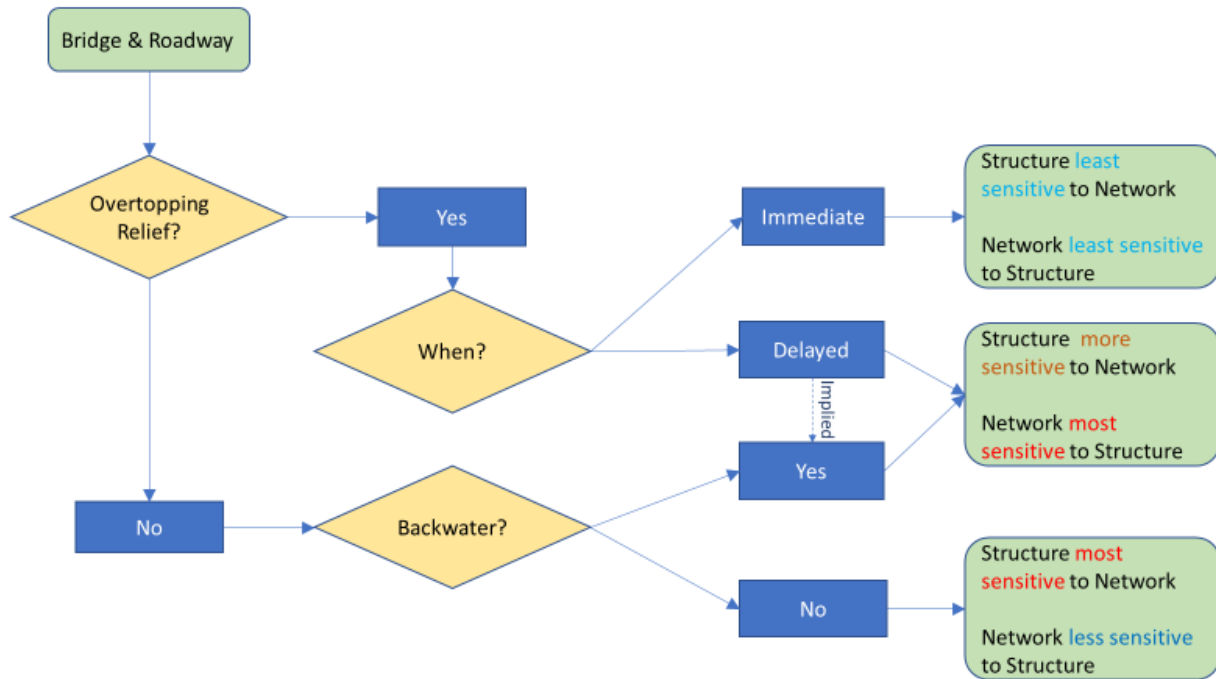
Figure 4.12: Simple flow chart identifying potential structure and network sensitivity. This does not account for geomorphological characteristics that may affect sensitivity, and requires knowledge of conditions at an individual bridge/road.

As floods increase in magnitude, the sensitivity of both the network and structures to perturbations will reduce, as most hydraulic controls will ultimately be overwhelmed. This is not to say that hazards are reduced, quite the opposite in fact, but that the proportional changes in WSE, discharge, and velocity caused by any perturbations will decrease once a threshold discharge is reached. For example, if a road is overtopped during a 100-year flood, but not in Q25, the network and structure sensitivity will be greater in the latter than the former, even though the overall hazard is less.

Vermont Railway Bridges 215, 219, and 220 have the most profound impacts on the network. To test more practical interventions than complete right-of-way removal, a series of simulations were run wherein each of these spans were increased by 50%, and their piers removed. Lengthening the spans of 219 and 220 result in increases in peak discharges up- and downstream, similar to their complete removal, but roughly 60-80% lesser in magnitude. However, while eliminating VTR 215 entirely caused reductions in peak discharge throughout the domain, increasing this structure's span results in increases in maximum flow—on top of the already magnified peak (Table 4.9). This means that taking advantage of the peak flow attenuation possible at this site requires a far more dramatic intervention than a 1.5× greater span alone.

Table 4.9: Discharge impact matrix for Q100, comparing removal with increasing spans of VTR Bridges 215, 219, 220 by 50%. Note: A lengthened span on VTR 215 further increases peak discharges, rather than the reduction observed when the structure was eliminated.

Δ Peak Discharge Q100 (cfs)		Impact on Bridge												
		Gorham	VTR 215	Depot	VTR 219	Kendall	Hammond	VTR 220	Syndicate	Union	Sanderson	Rt 73	VTR 228	LW	VTR 229
Existing		15,400	16,660	16,460	16,240	16,230	16,230	16,230	15,220	15,300	15,020	14,050	7,850	12,590	7,180
VTR 215	Removed	-27.2	190.8	-123.1	-110.2	-107.5	-108.6	-87.9	-77.2	-74.8	-71.8	-40.9	-17.4	-22.9	-1.6
	Increase Span	6.8	18.7	20.0	22.3	23.6	22.4	15.0	13.2	14.5	13.8	9.5	4.1	7.4	2.3
VTR 219	Removed	54.0	151.2	199.8	180.7	181.4	180.2	135.1	118.6	125.4	121.8	77.3	32.9	50.4	12.5
	Increase Span	12.4	32.7	43.3	44.3	45.8	44.6	33.3	28.9	30.1	28.8	18.2	7.9	12.8	3.3
VTR 220	Removed	20.7	60.6	100.8	126.1	128.9	127.8	173.8	152.3	158.5	153.9	105.2	43.9	69.2	18.1
	Increase Span	9.4	24.8	34.4	40.4	41.9	40.7	35.6	33.4	37.5	36.2	27.4	10.8	16.2	4.3

To determine the interactions between these three most-governing structures, simulations were run with both VTR 215 and 219 removed, and again with VTR 219 and 220 removed. The first combination tests the extent to which VTR 219 attenuates the increased peak discharge caused by VTR 215, some two miles upstream, under existing conditions. The second is intended to determine to what degree the attenuation provided by VTR 219 and 220, four miles apart, is additive. Results indicate that the impacts of removing the first pair is comparable to the sum of individual interventions; because of both the distance between structures and their control over the timing as well as the magnitude of peak discharge magnitude, the relationship is not strictly cumulative, though it trends this way with increasing downstream distance (Table 4.10). The second pair, VTR 219 and 220, which both attenuate flows, appear to have a more direct relationship, and the combined impacts are very close to the sum of the individuals (Table 4.11).

Table 4.10: Comparison of impacts of removing VTR Bridges 215, 219, and in combination, Q100. Combined effects are comparable to the sum of the individuals, but the nature of transient flow precludes a directly additive relationship.

Δ Peak Discharge Q100 (cfs)		Impact on Bridge												
		Gorham	VTR 215	Depot	VTR 219	Kendall	Hammond	VTR 220	Syndicate	Union	Sanderson	Rt 73	VTR 228	LW	VTR 229
Existing		15,400	16,660	16,460	16,240	16,230	16,230	16,230	15,220	15,300	15,020	14,050	7,850	12,590	7,180
Removed Bridge	VTR 215	-27.2	190.8	-123.1	-110.2	-107.5	-108.6	-87.9	-77.2	-74.8	-71.8	-40.9	-17.4	-22.9	-1.6
	VTR 219	54.0	151.2	199.8	180.7	181.4	180.2	135.1	118.6	125.4	121.8	77.3	32.9	50.4	12.5
	Both	17.5	354.4	39.5	36.1	36.6	35.5	26.3	22.7	31.8	31.0	25.1	11.1	22.2	10.0
	Sum	26.8	342.0	76.7	70.5	74.0	71.6	47.2	41.4	50.7	49.9	36.4	15.5	27.5	10.9

Table 4.11: Comparison of impacts of removing VTR Bridges 219, 220, and in combination, Q100. Combined effects are very comparable to the sum of the individuals.

Δ Peak Discharge Q100 (cfs)		Impact on Bridge												
		Gorham	VTR 215	Depot	VTR 219	Kendall	Hammond	VTR 220	Syndicate	Union	Sanderson	Rt 73	VTR 228	LW	VTR 229
Existing		15,400	16,660	16,460	16,240	16,230	16,230	16,230	15,220	15,300	15,020	14,050	7,850	12,590	7,180
Removed Bridge	VTR 219	54.0	151.2	199.8	180.7	181.4	180.2	135.1	118.6	125.4	121.8	77.3	32.9	50.4	12.5
	VTR 220	20.7	60.6	100.8	126.1	128.9	127.8	173.8	152.3	158.5	153.9	105.2	43.9	69.2	18.1
	Both	68.9	197.6	288.8	300.3	302.8	301.6	-530.1	268.9	281.4	273.7	180.0	74.4	116.9	28.8
	Sum	74.6	211.8	300.6	306.8	310.4	307.9	308.9	270.9	284.0	275.7	182.5	76.9	119.6	30.6

4.6.1 Uncertainty Analysis

Several factors contribute to uncertainty in these analyses. Foremost is implicit reliance on the accuracy of the VCGI hydro-flattened Lidar-DEM. Any applied corrections (i.e., bathymetry and bridge substructures) were based on measurements relative to this terrain model. When it comes to network-scale

impacts in extreme floods, the effect of any resulting error is minor, but not inconsequential. Ground-truthing and correction of surface elevations in densely vegetated floodplains would undoubtedly improve this model's accuracy. Errors in modeled absolute water surface elevation may be as high as two feet or more locally, and about one foot in most high-water mark locations near wetlands surveyed following TS Irene, and presumably are similar in synthetic storms. However, modeled WSE at gauge locations, where all flow is confined to the channel, matches observed stage within less than one foot for the majority of the duration of TS Irene. The implication is overestimation of vegetated floodplain elevation in the Lidar-derived terrain model. This is not surprising; based on observed vegetation and littoral debris density in the Otter Creek's floodplains, in all seasons, it is likely that only a handful of bona fide ground returns were obtained over thousands of acres of wetland, even though these were leaf-off scans. This is a well-known limitation of Lidar, and the result is spurious volume displacement in the floodplains, while vegetation-free roadway elevations are far more accurately modeled. This can also be anecdotally confirmed by the several culverts that do not fit between the road surface and adjacent floodplain elevations in the terrain model, based on their listed dimensions.

Resulting errors may cascade from there. First, maximum backwater volumes would necessarily be underestimated for all affected structures, which may affect the network's assessed sensitivity to some. Second, roadway overtopping may initiate prematurely in modeled storms, possibly leading to underestimation of channel velocity. Large discrepancies may be possible if overtopping relief occurs in the model when it does not in reality.

As far as the bridges themselves, considerable uncertainty is associated with structure sensitivity to network perturbations. Network sensitivity to a structure is less dependent on the detailed characteristics of the bridge than it is to the physical imposition of the crossing. On the other hand, structure sensitivity depends on much more than just its physical shape, and can only be properly quantified by detailed characterization of site-specific properties and more precise, rigorous, smaller-scale modeling. Computational demand necessitates a coarser-resolution model in this study than is appropriate to address individual structure sensitivity with any confidence. However, identification of the physical characteristics that affect a structure's propensity for sensitivity are nonetheless valid.

Manning's roughness coefficients, applied to the terrain boundary, are all within accepted ranges for their categories. There are, theoretically, infinite permutations of *n* values that could result in identical outflow hydrographs. The risk of selecting incorrect roughness values that incidentally yield an accurate solution is increased with the size of the domain. The effect here is unknown, although consistencies with intermediately-located high-water marks and typical *n* values indicate it is not likely a major concern.

Synthetic hydrographs were devised to propagate high peak discharge as far as reasonably possible downstream. In the flashier TS Irene, impacts of perturbations are more pronounced at nearby structures,

but attenuate more rapidly than in synthetic floods due to the greater proportion of flood volume that can be detained in storage at a given time. The unintended consequence is that these simulations may capture the farthest-reaching impacts at the expense of more significant localized impacts—this also highlights the value of transient analysis. The unpredictability of events that have rarely or never been observed hinders efforts to reliably model them. The floods modeled here will never be exactly realized; TS Irene may be an anomaly or the norm.

The possibility of structure failure is not addressed here. This may include a bridge itself, but in the context of Otter Creek, failure of a right-of-way berm may be of greater consequence to the network. Several structures, railway grades especially, can impound more volume than all seven actual dams on the Otter Creek. At certain stages of the flood wave, differences in potential in excess of three feet may occur due to flow constriction. This creates a significant hazard for a structure that was not engineered for this purpose. Paved roads and steel rails may make solid weir crests, but supercritical flows may quickly undermine these. Failure by piping is also a possible scenario, though this is unlikely due to the temporal constraints of a single flood. Chronic saturation may still lead to destabilization.

Obstruction by debris is a significant risk for most assessed bridges, and would almost certainly occur in modeled floods, as it did in TS Irene. Bridge piers at the VT Route 73 crossing routinely develop log/debris jams that span the entire channel in baseflow conditions, which present a hazard in flood conditions. This also occurs at Kendall Hill Rd. and Swamp Rd., which have piers in the channel as well. VTR Bridges 215, 219, and 220 are multi-span structures, though their piers are located such that they are more-or-less out of the channel in baseflow; they can still catch debris in high flows. Several other structures with minimal freeboard can also easily snag flotsam, and do. Several of the largest logjams on the Otter Creek are so substantial that they have become permanent and are forcing lateral channel migration. The dozens of smaller jams (which still may contain several full >2 foot diameter trees) are more mobile and susceptible to disruption by ice, and either migrate into a permanent jam or snag on bridge piers in common high flows (e.g., annual spring floods). This is a site-specific hazard that can drastically impact a bridge's sensitivity.

5. CONCLUSIONS AND RECOMMENDATIONS

From this research, several recommendations can be made regarding network-scale bridge-stream interactions, and flood hazard mitigation in the Otter Valley. Utilization of large-scale two-dimensional, transient hydraulic models can provide valuable insights into network resiliency and response to proposed infrastructure improvements. Once this has been established, and a structure's area of influence defined, a smaller-scale, finer-resolution model can then be used for detailed analyses. These 2D models may also be used to produce high-quality visualizations and animations that may enhance understanding among a lay audience. A further advantage of a network-scale model analysis is that stream-gauge data available within the watershed may be used for calibration and more accurate understanding of the potential conditions encountered at locations of interest. Floodplains and structures may contribute to considerably different peak flows than are estimated with standard regressions (Table 4.3), and network impacts, even between adjacent structures, cannot be accurately determined under steady-state conditions. Synthetic hydrographs can be created in place of or in addition to stream gauge records to analyze transient flow dynamics. For a given peak discharge magnitude, the effects of backwater or floodplain storage are maximized with steeper, flashier hydrographs; hydraulic connectivity between structures is maximized with a broader, more massive hydrograph.

Calibration of the Otter Creek model to observed discharge in TS Irene is a significant contributor to this study. However, only a handful of Vermont rivers have multiple flow gauges, which may complicate efforts to calibrate and validate models in other watersheds by the means presented here. Deployment of additional gauging stations in strategic locations may provide valuable information both for this purpose and many others in future flood events. Structures may have a strong influence on the local stage-discharge relationship, which should be considered for gauge placement. Flow data from hydro-power stations and flood control dams may be available on other rivers as well, and could be a useful supplement to USGS stations.

The proportion of river systems with appreciable floodplain access is steadily increasing in Vermont, due to ongoing rehabilitation and resiliency improvement projects. The Otter Creek is somewhat unique in terms of extent and connectivity of floodplain, but nearly all rivers in the state have at least some floodplain access, and often these are interrupted by infrastructure. Allowance of overbank flow can be the most effective strategy for reducing velocities through a structure. Bridges that constrict the river channel may naturally be targeted for replacement, but if the approach roadway traverses the floodplain, a far more economical solution may be installation of relief structures—assuming the bridge is stable for bankfull discharge. If the road is a critical link in transportation or life safety networks, a handful of culverts are insufficient for this purpose; substantial supplemental conveyance is necessary. If the roadway is of low importance (e.g., low traffic, short detour length), grade reduction to allow overtopping may even be

practical. Strategic loss of service in extreme floods may be a suitable strategy to reduce the risk of bridge failure at marginal cost. Overbank relief may also be employed in combination with increasing a bridge span, potentially lowering the overall cost of crossing improvements. Further, these insights emphasize the value of river restoration, especially in the vicinity of bridges; rehabilitation of incised or entrenched streams and reconnection to their floodplains may dramatically enhance the benefits of additional relief provisions.

These sorts of projects are generally targeted at improving hydraulics at an individual bridge. Depending on the changes made, and characteristics of surrounding bridges, additional analyses may be prudent. It is possible for a perturbation to have potentially positive (discharge reduction), potentially negative (discharge increased), or inconsequential impacts on other structures. Similarly, these receiving structures may experience these impacts with varying degrees of sensitivity (Figure 4.12). Velocity has been used here as a proxy for structure sensitivity, but various foundation and sediment characteristics will dictate how changes in velocity may actually affect structure stability. Wholesale removal of bridges and roadways was the primary perturbation tested; this results in the most dramatic changes and most conservative scenarios possible. More practical interventions, such as increasing spans to 1.5× bankfull, cause less substantial changes, though they are nonetheless measurable. The overall shallow-slope of the Otter Valley does not generate especially high velocities, but, for example, it may be possible for perturbations to require re-sizing of channel stabilizing stone fill from Type I to Type II (VTrans, 2015).

Specific to the assessed bridges on the Otter Creek, analyses suggest prioritization of Vermont Railway Bridge 215, Leicester-Whiting Road, and Vermont Route 73 for rehabilitation, all else being equal. Sufficiently increasing conveyance at these structures will reduce velocities therein, result in a decrease in peak discharge and velocity at downstream structures, and reduce backwater inundation upstream. These are a win-win. On the other hand, Vermont Railway Bridges 219 and 220 provide the most flow attenuation, and increased conveyance at these will result in increased peak discharges, and potentially greater velocities, at downstream structures. Thus improvement of local hydraulics may degrade conditions at other bridges, and further analysis of the network response should be included in planning and design. Elimination of tailwater controls can also cause increased flows at upstream structures, and should be considered where applicable. Provision of relief to Hammond Covered Bridge, or further raising the structure, may help preserve this historic bridge, although it has no value to the transportation network other than as a pedestrian crossing. This and the remaining eight assessed bridges may be adjusted without significant consequence to the network, provided that these adjustments increase conveyance rather than reduce it.

6. REFERENCES

Abdulkareem, M., Elkadi, H., (2018). "From engineering to evolutionary, an overarching approach in identifying the resilience of urban design to flood" *International Journal of Disaster Risk Reduction* 28: 176-190

Anderson, I., Rizzo, D.M., Huston, D.R., and Dewoolkar, M. M., (2017a). "Analysis of bridge and stream conditions of over 300 Vermont bridges damaged in Tropical Storm Irene" *Structure and Infrastructure Engineering* 13.11: 1437-1450.

Anderson, I., Rizzo, D.M., Huston, D.R., and Dewoolkar, M. M., (2017b). "Stream Power Application for Bridge-Damage Probability Mapping Based on Empirical Evidence from Tropical Storm Irene" *Journal of Bridge Engineering* 22.5: 12p.

Acrement Jr., G.J., and Schneider, V.R., (1987). Roughness coefficients for densely vegetated flood plains: USGS Water-Resources Investigations Report 83-4247, 71p., available at https://pubs.er.usgs.gov/publication/wri834247

Acrement Jr., G.J., and Schneider, V.R., (1989). Guide for selecting Manning's roughness coefficients for natural channels and flood plains: USGS Water Supply Paper 2339, 38p., available at https://pubs.er.usgs.gov/publication/wsp2339

Arneson, L. A., Zevenbergen, L. W., Lagasse, P. F., and Clopper, P. E. (2012). "Evaluating scour at bridges." FHWA-HIF-12-003, HEC-18, 340p.

Cheng, C., Ethan Yang, Y.C., Ryan, R., et al., (2017). "Assessing climate change-induced flooding mitigation for adaptation in Boston's Charles River watershed, USA" *Landscape and Urban Planning* 167: 25-36

Chow, V.T., (1959). *Open Channel Hydraulics*, Blackburn Press, Caldwell, NJ.

Courant, R., Friedrichs, K., Lewy, H., (1928). "On the partial difference equations of mathematical physics" *Mathematische Annalen* 100: 32-74.

FHWA (1995). "Recording and coding guide for the structure inventory and appraisal of the nation's bridges." FHWA-PD-96-001, U.S. Dept. of Transportation, Washington, D.C.

FHWA (2012). "Bridge Inspector's Reference Manual." FHWA-NHI-12-049, U.S. Dept. of Transportation, Washington D.C.

Gartner, J.D., Magilligan, F.J., Renshaw, C.E., (2015). "Predicting the type, location and magnitude of geomorphic responses to dam removal: Role of hydrologic and geomorphic constraints" *Geomorphology* 251: 20-30.

Guilbert, J., Betts, A. K., Rizzo, D. M., Beckage, B., and Bomblies, A., (2015). "Characterization of increased persistence and intensity of precipitation in the northeastern United States" *Geophysical Research Letters* 42.6: 1888-1893.

Gumbel, E.J., (1941). "The return period of flood flows" *The Annals of Mathematical Statistics* 12.2: 163-190.

Horton, R., Yohe, G., Easterling, W., Kates, R., Ruth, M., Sussman, E., Whelchel, A., Wolfe, D., and Lipschultz, F. (2014). "Ch. 16: Northeast, climate change impacts in the United States." *The Third National Climate Assessment*, edited by J. M. Melillo, T. C. Richmond, and G. W. Yohe, pp. 371–395, U.S. Global Change Research Program, Washington, D. C., doi:10.7930/J0SF2T3P.

Hodgson, M.E., Jenson, J., Raber, G., et al., (2005) "An evaluation of lidar-derived elevation and terrain slope in leaf-off conditions" *Photogrammetric Engineering and Remote Sensing* 71.7: 817-823.

Homer, C.G., Dewitz, J.A., Yang, L., Jin, S., Danielson, P., Xian, G., Coulston, J., Herold, N.D., Wickham, J.D., and Megown, K., (2015). "Completion of the 2011 National Land Cover Database for the conterminous United States-Representing a decade of land cover change information" *Photogrammetric Engineering and Remote Sensing* 81.5: 345-354.

Johnson, P.A., (2002) "Incorporating road crossings into stream and river restoration projects" *Ecological Restoration* 20.4: 270-277.

Johnson, P.A., Hey, R.D., Brown, E.R., Rosgen, D.L., (2002) "Stream restoration in the vicinity of bridges" *Journal of the American Water Resources Association* 38.1: 55-67.

Johnson, P.A., (2006). "Physiographic characteristics of bridge-stream intersections" *River Research and Applications* 22: 617-630.

Kline, M. and Cahoon, B., (2010). "Protecting river corridors in Vermont" *Journal of the American Water Resources Association* 46.2: 227-236.

Kosicki, A.J. and Davis, S. R., (2001). "Consideration of stream morphology in culvert and bridge design" *Transportation Research Record* 1743: 57-59, Paper No. 01-2466.

Lagasse, P.F., Byars, L.W., et al., (2009). "Bridge scour and stream instability countermeasures: Experience, selection, and design guidance 3e, FHWA-NHI-09-111, HEC-23, 255p.

Lagasse, P.F., Schall, J.D., Johnson, F., et al., (2012). Stream stability at highway structures 4e, FHWA-HIF-12-004, HEC-20, 328p.

McEnroe, B.M., (2006). Downstream effects of culvert and bridge replacement. Kansas Department of Transportation Report K-TRAN: KU-04-9. 60p.

Medalie, L., and Olson, S.A., (2013). High-water marks from flooding in Lake Champlain from April through June 2011 and Tropical Storm Irene in August 2011 in Vermont: U.S. Geological Survey Data Series 763, 11 p., available at http://pubs.usgs.gov/ds/763/

Melillo, J. M., Richmond, T.C., and Yohe, G. W. (Eds.) (2014). "Climate Change Impacts in the United States: The Third National Climate Assessment". U.S. Global Change Research Program, 841 pp. Doi: 10.7930/J0Z31WJ2.

Nash, J.E., and Sutcliffe, J.V., (1970), "River flow forecasting through conceptual models" *Journal of Hydrology* 10: 282-290.

National Weather Service Burlington, VT, (2011). Preliminary Hurricane/Tropical Storm Irene Weather Summary for the North Country, available at https://www.weather.gov/media/btv/events/Irene2011/Irene2011.pdf

Olson, S.A. (2014) "Estimation of flood discharges at selected annual exceedance probabilities for unregulated, rural streams in Vermont, with a section on Vermont regional skew regression, by Veilleux, A.G." *US Geological Survey Scientific Investigations Report 2014-5078*, 27p.

Perica, S., Pavlovic, S., St. Laurent, M., Trypaluk, C., et al. (2015) NOAA Atlas 14: Precipitation-Frequency Atlas of the United States Vol. 10 Version 2.0: Northeastern States. Hydrometeorological Design Studies Center, National Oceanic and Atmospheric Administration, US Dept. of Commerce.

State of Vermont, (2012). Tropical Storm Irene after action report/improvement plan. FOUO.

USACE (2018) Hydraulic Engineering Center River Analysis System (HEC-RAS) v5.0.5 [Computer Software]

USACE HEC (2016a) "HEC-RAS User's Manual" CPD-68 v5.0, Davis, CA. 960p.

USACE HEC (2016b) "HEC-RAS 2D Modeling User's Manual" CPD-68A v5.0, Davis, CA. 171p.

USACE HEC (2016c) "HEC-RAS Hydraulic Reference Manual" CPD-69 v5.0, Davis, CA. 547p.

USACE HEC (2018) "Supplemental to HEC-RAS Version 5.0 User's Manual" CPD-68D v5.0.4, Davis, CA. 74p.

U.S. Geological Survey, (2018a). National Water Information System data available on the World Wide Web (USGS Water Data for the Nation), USGS Gauge 04282000 Otter Creek at Rutland, VT, http://waterdata.usgs.gov/nwis/inventory/?site_no=04282000

U.S. Geological Survey, (2018b). National Water Information System data available on the World Wide Web (USGS Water Data for the Nation), USGS Gauge 04282500 Otter Creek at Middlebury, VT, http://waterdata.usgs.gov/nwis/inventory/?site_no=04282500

U.S. Geological Survey, (2018c). National Water Information System data available on the World Wide Web (USGS Water Data for the Nation), USGS Gauge 04282525 New Haven River at Brooksville near Middlebury, VT, http://waterdata.usgs.gov/nwis/inventory/?site_no=04282525

State of Vermont, (2018). Interactive map database of Vermont culverts, Vermont Agency of Transportation and Vermont Regional Planning Commissions, available at http://www.vtculverts.org

Vermont Agency of Transportation, (2015) *Hydraulics Manual*. Technical Manual, 201p.

Watson, K.B., Ricketts, T., Galford, G., et al., (2016). "Quantifying flood mitigation services: The economic value of Otter Creek wetlands and floodplains to Middlebury, VT" *Ecological Economics* 130: 16-24.

Wu, W., (2008). *Computational River Dynamics*, Taylor & Francis, London.

7. APPENDIX

Table 7.1: Relevant asset inventory identifiers and geographical locations of assessed bridges. River station measured downstream from Proctor Falls.

Road/Bridge	Route Name	Town	Local Bridge ID	BIS ID	VTR Asset ID	Location (VT State Plane)		River Station [Proctor] (ft)
						X (m)	Y (m)	
Gorham Bridge	C3006	Proctor	4	101118000411181	N/A	456,657	131,230	10,700
VTR 215	VTR Northern	Pittsford	215	N/A	B-05-06-03/04	456,721	133,795	22,160
Depot Hill Rd	C3023	Pittsford	33	101116003311161	N/A	456,260	134,504	27,180
VTR 219	VTR Northern	Pittsford	219	N/A	B-05-06-06/07	455,550	135,368	35,070
Kendall Hill Rd	FAS 0155	Pittsford	12	200155001211162	N/A	455,428	135,684	36,190
Hammond Bridge	N/A	Pittsford	Historic Structure, closed to vehicle traffic			455,399	135,753	36,420
VTR 220	VTR Northern	Pittsford	220	N/A	B-05-06-08/09	454,921	139,100	56,100
Syndicate Rd/ Carver St	C3042	Brandon	25	101102002511021	N/A	453,960	139,836	60,400
Union St	C2005	Brandon	11	101102001111021	N/A	451,928	142,248	75,240
Sanderson Bridge	C2004	Brandon	12	101102001211021	N/A	450,769	143,442	82,750
VT Route 73	VT73	Sudbury	5	200158000511232	N/A	447,376	145,834	103,110
VTR 228	VTR Northern	Leicester	228	N/A	B-05-07-03	447,827	150,674	120,610
Leicester-Whiting Rd	FAS 0160	Leicester	6	200160000601092	N/A	447,884	150,779	121,000
VTR 229	VTR Northern	Leicester	229	N/A	B-05-07-04	447,200	152,347	127,600

Table 7.2: Waterway adequacy rating definitions (FHWA, 2012).

| Rating | | | Description |
Express-ways	Collectors	Locals	
9	9	9	Bridge deck and roadway approaches above flood water elevations (high water). Chance of overtopping is remote.
8	8	8	Bridge deck above roadway approaches. Slight chance of overtopping roadway approaches.
6	6	7	Slight chance of overtopping bridge deck and roadway approaches.
4	5	6	Bridge deck above roadway approaches. Occasional overtopping of roadway approaches with insignificant traffic delays.
3	4	5	Bridge deck above roadway approaches. Occasional overtopping of roadway approaches with significant traffic delays.
2	3	4	Occasional overtopping of roadway approaches with significant traffic delays.
2	2	3	Frequent overtopping of bridge deck and roadway approaches with significant traffic delays.
2	2	2	Occasional or frequent overtopping of bridge deck and roadway approaches with severe traffic delays.
0	0	0	Bridge closed

Table 7.3: Channel rating definitions (FHWA, 2012).

Rating	Description
9	There are no noticeable or noteworthy deficiencies which affect the condition of the channel.
8	Banks are protected or well vegetated. River control devices such as spur dikes and embankment protection are not required or are in a stable condition.
7	Bank protection is in need of minor repairs. River control devices and embankment protection have a little minor damage. Banks and/or channel have minor amounts of drift.
6	Bank is beginning to slump. River control devices and embankment protection have widespread minor damage. There is minor stream bed movement evident. Debris is restricting the channel slightly.
5	Bank protection is being eroded. River control devices and/or embankment have major damage. Trees and brush restrict the channel.
4	Bank and embankment protection is severely undermined. River control devices have severe damage. Large deposits of debris are in the channel.
3	Bank protection has failed. River control devices have been destroyed. Stream bed aggradation, degradation or lateral movement has changed the channel to now threaten the bridge and/or approach roadway.
2	The channel has changed to the extent the bridge is near a state of collapse.
1	Bridge closed because of channel failure. Corrective action may put back in light service.
0	Bridge closed because of channel failure. Replacement necessary.

Table 7.4: Scour rating definitions (FHWA, 1995).
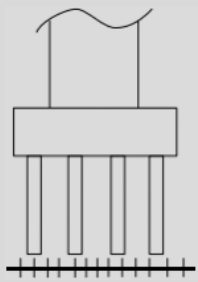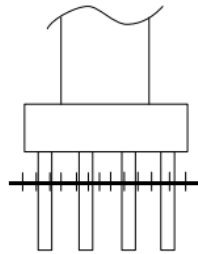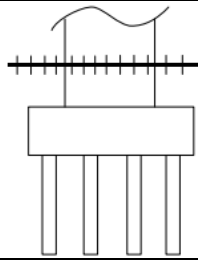
Rating	Description	Notes	Example
U	No information on the foundation is available – Unknown foundation.	Bridges with U are expected to be added to those considered scour critical.	
0	Bridge is scour critical. Bridge has failed and is closed to traffic.	Bridges with ratings 0 through 3 are considered scour critical.	
1	Bridge is scour critical; field review indicates that failure of piers/abutments is imminent. Bridge is closed to traffic.		
2	Bridge is scour critical; field review indicates that extensive scour has occurred at bridge foundations. Immediate action is required to provide scour countermeasures.		
3	Bridge is scour critical; bridge foundations determined to be unstable for calculating scour conditions.		
4	Bridge foundations determined to be stable for calculated scour; field review indicates action required to protect foundations from additional erosion.	Bridges with ratings 4 through 9 are considered non-scour critical.	
5	Bridge foundations determined to be stable for calculated scour conditions; scour within limits of footing or piles.		
6	Scour calculation/evaluation has not been made.		
7	Countermeasures have been installed to correct previously existing scour. Bridge is no longer scour critical.		
8	Bridge foundations determined to be stable for calculated scour conditions; calculated scour is above top of footing. If bridge was screened or studied by experts and found to be low risk, it should fall into this category.		
9	Bridge foundations (including piles) well above flood water elevations.		

Table 7.5: Q500 discharge impact matrix.

Δ Peak Discharge Q500 (cfs)		Impact on Bridge													
		Gorham	RR 215	Depot	RR 219	Kendall	Hammond	RR 220	Syndicate	Union	Sanderson	Rt 73	RR 228	LW	RR 229
Existing		18,240	20,400	19,950	19,690	19,680	19,680	18,880	18,170	18,660	18,350	15,830	9,850	16,460	6,140
Removed Bridge	RR 215	-28.1	80.9	-127.5	-120.0	-119.3	-120.8	-94.7	-80.6	-84.2	-80.1	-42.4	-21.8	-29.3	-8.9
	RR 219	77.4	235.6	260.4	202.9	202.7	201.2	155.4	129.0	154.4	149.1	86.3	39.8	59.8	19.1
	RR 220	32.5	90.1	151.7	164.8	166.9	165.6	143.7	105.8	137.1	135.8	104.0	49.6	82.3	28.4
	Rt 73	11.4	32.0	29.5	28.1	29.7	28.2	19.3	23.1	20.2	11.5	-1270.1	-35.0	-55.7	-26.2
	LW	11.2	31.7	29.2	28.0	29.6	28.1	20.1	18.1	32.1	43.3	22.3	-685.2	378.9	-585.6

Table 7.6: Q100 discharge impact matrix.

Δ Peak Discharge Q100 (cfs)		Impact on Bridge													
		Gorham	RR 215	Depot	RR 219	Kendall	Hammond	RR 220	Syndicate	Union	Sanderson	Rt 73	RR 228	LW	RR 229
Existing		15,400	16,660	16,460	16,240	16,230	16,230	16,230	15,220	15,300	15,020	14,050	7,850	12,590	7,180
Removed Bridge	Gorham	-2.9	17.9	22.5	24.7	26.1	24.8	17.2	15.1	16.7	15.9	10.8	4.8	8.2	2.5
	RR 215	-27.2	190.8	-123.1	-110.2	-107.5	-108.6	-87.9	-77.2	-74.8	-71.8	-40.9	-17.4	-22.9	-1.6
	Depot	7.4	12.4	32.9	17.7	19.0	17.7	10.2	9.0	9.7	9.1	4.2	0.9	1.2	-0.1
	RR 219	54.0	151.2	199.8	180.7	181.4	180.2	135.1	118.6	125.4	121.8	77.3	32.9	50.4	12.5
	Kendall	12.6	34.0	43.7	45.4	46.6	45.2	33.5	29.3	30.6	29.1	18.7	8.1	13.2	3.3
	Hammond	10.6	26.4	31.6	32.6	34.0	38.0	23.9	21.4	23.3	22.2	15.2	6.9	10.6	3.5
	RR 220	20.7	60.6	100.8	126.1	128.9	127.8	173.8	152.3	158.5	153.9	105.2	43.9	69.2	18.1
	Syndicate	8.9	21.7	27.7	30.2	31.6	30.3	16.8	54.8	15.8	15.1	14.1	6.7	12.6	4.8
	Union	8.2	19.6	24.6	26.7	28.1	26.8	16.4	19.1	10.5	4.8	-1.4	-3.7	-5.7	-2.4
	Sanderson	8.0	19.9	26.1	29.7	31.1	29.8	28.6	34.9	22.6	162.8	3.0	3.4	11.4	7.2
	Rt 73	7.8	18.5	23.2	25.3	26.7	25.4	17.0	18.0	13.0	3.4	-952.9	-48.8	-78.6	-27.9
	RR 228	7.7	19.0	23.9	26.1	27.5	26.2	18.3	16.1	18.4	20.0	90.8	805.9	27.8	354.9
	LW	7.7	19.0	23.9	26.1	27.4	26.2	18.3	16.1	22.7	33.6	108.1	-767.0	478.2	-657.1
	RR 229	7.7	19.1	23.8	26.1	27.4	26.2	18.3	16.0	17.6	16.9	0.9	245.0	125.8	366.9

Table 7.7: Q50 discharge impact matrix.

Δ Peak Discharge Q50 (cfs)		Impact on Bridge													
		Gorham	RR 215	Depot	RR 219	Kendall	Hammond	RR 220	Syndicate	Union	Sanderson	Rt 73	RR 228	LW	RR 229
Existing		13,720	14,100	14,100	13,900	13,880	13,880	13,270	13,120	12,970	12,730	11,750	7,100	10,840	6,140
Removed Bridge	Gorham	-4.7	11.1	20.5	19.0	20.1	19.0	14.1	12.0	12.7	12.2	7.3	3.2	5.0	1.4
	RR 215	-21.7	310.8	-123.6	-112.3	-110.1	-111.0	-73.8	-67.2	-55.0	-51.8	-17.2	-7.8	0.3	8.5
	Depot	6.6	2.9	35.5	11.7	12.7	11.6	6.2	4.6	4.2	3.7	-0.6	-0.9	-2.5	-1.0
	RR 219	39.0	88.5	145.6	139.8	139.9	138.7	99.2	90.6	85.8	82.6	46.9	20.0	30.5	5.4
	Kendall	9.1	20.4	36.0	34.8	35.7	34.5	24.7	21.1	21.4	20.5	11.2	5.0	6.9	1.4
	Hammond	8.5	17.9	31.0	28.7	29.8	32.6	20.8	17.7	18.6	17.8	10.6	4.8	7.0	1.5
	RR 220	13.5	36.4	79.3	98.8	101.0	100.1	118.1	109.0	103.4	99.8	62.6	26.1	43.2	8.5
	Syndicate	7.1	14.7	27.5	26.7	27.8	26.7	17.9	45.1	14.7	14.3	13.6	6.6	13.2	4.8
	Union	6.4	13.0	23.9	22.4	23.5	22.5	16.1	14.2	16.9	2.5	2.0	-0.6	1.3	1.5
	Sanderson	6.0	11.9	22.2	21.3	22.4	21.3	26.2	26.9	32.3	176.9	14.1	6.3	18.4	8.5
	Rt 73	6.1	11.1	21.0	18.9	19.9	18.9	12.4	11.1	8.2	-1.6	-757.3	-49.7	-81.5	-20.3
	RR 228	6.0	11.9	21.7	20.0	21.1	20.0	14.7	12.7	13.3	13.0	68.1	828.2	47.8	359.7
	LW	6.0	11.9	21.6	20.0	21.1	20.0	14.7	12.7	13.5	15.1	183.2	-734.9	598.3	-639.9
	RR 229	6.0	11.8	21.6	20.0	21.1	20.0	14.6	12.6	13.0	12.5	4.7	10.3	111.4	377.8

Table 7.8: Q25 discharge impact matrix.

Δ Peak Discharge Q25 (cfs)		Impact on Bridge													
		Gorham	RR 215	Depot	RR 219	Kendall	Hammond	RR 220	Syndicate	Union	Sanderson	Rt 73	RR 228	LW	RR 229
Existing		12,070	12,320	12,480	12,280	12,270	12,270	11,570	11,440	11,230	11,020	10,130	6,130	8,590	5,260
Removed Bridge	Gorham	-4.7	10.2	18.9	17.9	18.7	17.7	12.6	12.2	10.3	10.0	7.8	2.0	3.8	0.9
	RR 215	-13.1	462.1	-108.7	-98.5	-97.3	-98.2	-53.5	-42.4	-26.5	-23.4	-16.9	7.2	16.6	12.1
	Depot	5.1	-0.7	37.4	9.9	10.9	9.9	5.1	4.7	3.4	3.0	1.8	-0.3	-0.4	-0.3
	RR 219	28.5	46.8	130.8	121.4	121.1	120.1	82.9	76.1	64.9	61.7	49.8	11.4	20.5	2.6
	Kendall	6.5	12.0	31.7	31.0	30.7	29.6	20.1	19.1	15.7	15.1	11.8	2.7	4.8	0.6
	Hammond	6.0	9.4	28.9	29.1	29.0	30.9	18.6	17.7	14.8	14.3	11.1	2.6	4.8	0.9
	RR 220	8.9	26.5	64.1	81.6	83.5	82.6	100.2	92.9	81.9	78.1	63.5	16.7	30.4	5.0
	Syndicate	5.4	12.8	25.2	26.5	27.5	26.5	18.0	47.7	15.1	15.0	12.9	6.8	12.7	5.2
	Union	4.8	11.5	21.9	21.9	22.8	21.9	16.0	16.8	22.6	0.8	-3.3	2.9	6.1	4.6
	Sanderson	4.5	10.5	19.5	18.6	19.5	18.5	21.8	26.7	38.2	175.2	15.6	10.3	20.2	9.8
	Rt 73	4.7	9.6	19.2	18.3	19.0	18.0	9.3	9.3	7.5	3.2	-730.6	-45.1	-75.6	-11.1
	RR 228	4.5	10.5	19.4	18.4	19.2	18.2	12.8	12.3	10.5	10.1	18.8	739.0	92.1	286.1
	LW	4.5	10.5	19.4	18.4	19.2	18.2	12.8	12.3	10.6	10.3	138.8	-614.5	616.8	-639.2
	RR 229	4.5	10.5	19.4	18.4	19.2	18.2	12.6	12.1	10.2	9.6	16.0	-62.6	-40.4	339.5

Table 7.9: TS Irene discharge impact matrix.

Δ Peak Discharge TS Irene (cfs)	Impact on Bridge													
	Gorham	RR 215	Depot	RR 219	Kendall	Hammond	RR 220	Syndicate	Union	Sanderson	Rt 73	RR 228	LW	RR 229
Existing	17,620	17,660	17,370	17,050	17,020	17,020	15,840	15,480	15,290	15,000	13,530	7,350	11,440	6,620
Gorham	-2.9	33.4	36.9	33.4	34.9	33.6	19.4	17.2	15.5	15.2	11.6	3.6	6.6	2.3
RR 215	-32.5	173.4	-164.6	-157.1	-154.4	-155.6	-68.5	-59.6	-39.4	-37.2	-24.3	-1.9	12.3	11.8
Depot	13.1	30.7	50.1	27.9	29.4	28.1	19.1	17.1	16.9	17.0	14.0	5.2	10.1	3.9
RR 219	75.7	238.9	297.0	267.9	268.0	266.5	136.6	119.1	103.3	101.0	76.8	21.3	31.9	8.8
Kendall	17.1	55.6	64.4	61.1	62.2	60.7	34.9	29.8	25.9	25.8	19.4	5.1	8.4	2.4
Hammond	16.1	49.0	52.3	45.9	47.4	51.5	26.1	22.6	20.7	20.5	16.0	5.0	9.3	3.0
RR 220	13.8	64.3	117.8	148.9	152.2	151.1	204.5	178.3	158.0	154.8	119.3	34.8	54.6	15.4
Syndicate	12.2	40.5	45.8	41.4	42.9	41.6	22.4	60.0	21.3	21.9	19.6	7.0	14.8	6.1
Union	11.7	35.8	40.7	38.8	40.3	39.0	23.8	26.2	9.1	2.6	-1.2	1.8	7.8	4.2
Sanderson	11.5	35.1	38.2	34.7	36.1	34.8	32.7	40.5	44.4	189.9	10.9	11.7	32.2	15.3
Rt 73	11.5	35.2	38.5	35.0	36.5	35.2	23.1	23.5	29.2	17.8	-996.4	-38.4	-40.5	-5.0
RR 228	11.5	35.0	38.2	34.6	36.0	34.7	20.2	17.9	16.0	15.8	28.5	831.0	75.2	395.1
LW	11.5	35.1	38.2	34.6	36.0	34.7	20.2	17.9	15.8	15.2	140.7	-644.2	608.2	-652.1
RR 229	11.5	35.0	38.2	34.6	36.1	34.7	20.0	17.8	15.8	14.9	1.9	193.4	146.4	346.9

Table 7.10: Q500 velocity impact matrix.

Δ Peak Velocity Q500 (fps)	Impact on Bridge													
	Gorham	RR 215	Depot	RR 219	Kendall	Hammond	RR 220	Syndicate	Union	Sanderson	Rt 73	RR 228	LW	RR 229
Existing	5.174	4.885	1.732	5.656	8.353	6.779	7.064	2.431	4.499	5.612	3.369	4.956	5.755	3.922
RR 215	0.254	-3.035	0.001	-0.001	-0.043	-0.028	-0.020	-0.008	-0.010	-0.015	-0.003	-0.014	-0.015	0.254
RR 219	0.027	0.086	0.045	-0.653	0.035	0.060	0.027	0.012	0.019	0.022	0.002	0.016	0.023	0.027
RR 220	0.004	0.010	0.012	0.094	0.124	0.120	-2.468	0.010	0.016	0.019	0.001	0.014	0.023	0.004
Rt 73	0.007	0.003	0.010	0.025	0.004	0.011	0.006	0.005	0.045	0.134	-1.835	-0.017	-0.020	0.007
LW	0.006	0.001	0.008	0.024	0.002	0.010	0.001	0.001	0.008	0.019	0.111	-0.175	-1.954	0.006

Table 7.11: Q100 velocity impact matrix.

Δ Peak Velocity Q100 (fps)	Impact on Bridge													
	Gorham	RR 215	Depot	RR 219	Kendall	Hammond	RR 220	Syndicate	Union	Sanderson	Rt 73	RR 228	LW	RR 229
Existing	4.994	4.836	1.857	5.191	7.458	6.073	6.464	2.697	4.198	5.296	3.710	4.779	5.337	3.579
Gorham	-0.758	-0.003	0.005	-0.002	0.001	0.006	-0.001	0.003	0.001	0.003	-0.002	0.001	0.002	0.002
RR 215	0.223	-2.689	-0.019	-0.031	-0.045	-0.033	-0.030	-0.001	-0.012	-0.013	-0.006	-0.012	-0.017	-0.001
Depot	0.013	0.025	-0.269	-0.003	-0.001	0.004	-0.003	0.004	0.000	0.003	-0.002	-0.001	0.000	0.001
RR 219	0.019	0.069	0.031	-0.602	0.028	0.052	0.031	0.007	0.015	0.022	0.000	0.014	0.021	0.006
Kendall	-0.001	0.000	0.006	0.017	-0.584	-0.023	0.003	0.003	0.003	0.006	-0.002	0.002	0.004	0.002
Hammond	0.000	0.004	0.007	0.010	0.015	-0.690	0.000	0.004	0.002	0.005	-0.002	0.001	0.003	0.002
RR 220	-0.001	0.000	0.006	0.053	0.094	0.087	-2.246	-0.099	0.018	0.025	-0.001	0.017	0.026	0.008
Syndicate	0.005	-0.001	0.008	0.004	0.010	0.013	0.010	-0.146	0.000	0.002	-0.005	0.000	0.001	0.002
Union	0.005	0.000	0.011	0.001	0.005	0.009	0.004	0.103	-1.325	0.003	-0.015	-0.004	-0.005	0.000
Sanderson	0.004	-0.001	0.007	0.000	0.003	0.008	0.009	0.034	0.129	-1.049	0.003	-0.004	-0.005	0.002
Rt 73	0.005	0.001	0.012	-0.001	0.003	0.007	0.002	0.104	0.042	0.123	-2.086	-0.028	-0.037	-0.009
RR 228	0.004	-0.002	0.005	-0.002	0.001	0.006	-0.001	0.003	0.001	0.004	0.001	-1.560	0.014	0.125
LW	0.004	-0.002	0.005	-0.002	0.001	0.006	-0.001	0.004	0.002	0.008	0.024	-0.278	-1.785	-0.282
RR 229	0.004	-0.002	0.005	-0.002	0.001	0.006	-0.001	0.004	0.001	0.004	0.008	-0.016	0.111	-1.385

Table 7.12: Q50 velocity impact matrix.

Δ Peak Velocity Q50 (fps)	Impact on Bridge													
	Gorham	RR 215	Depot	RR 219	Kendall	Hammond	RR 220	Syndicate	Union	Sanderson	Rt 73	RR 228	LW	RR 229
Existing	4.888	4.855	2.067	4.774	6.838	5.551	5.820	3.146	3.973	5.003	3.826	4.508	4.972	3.312
Gorham	-0.764	-0.003	0.007	0.000	-0.003	0.006	-0.003	0.001	0.001	0.002	0.004	0.002	0.003	-0.247
RR 215	0.222	-2.457	-0.021	-0.032	-0.054	-0.039	-0.031	-0.007	-0.010	-0.014	-0.001	-0.005	-0.005	0.000
Depot	0.011	0.028	-0.334	0.000	-0.004	0.004	-0.005	-0.003	0.001	0.000	0.003	0.000	0.001	-0.002
RR 219	0.052	0.121	0.022	-0.476	0.017	0.043	0.024	0.010	0.012	0.016	0.008	0.010	0.012	0.001
Kendall	0.001	0.000	0.006	0.014	-0.465	-0.016	0.001	0.001	0.003	0.003	0.005	0.003	0.004	-0.001
Hammond	0.002	0.004	0.005	0.011	0.011	-0.578	0.000	0.002	0.002	0.003	0.004	0.003	0.004	-0.001
RR 220	0.004	-0.001	0.005	0.042	0.067	0.065	-1.874	-0.103	0.013	0.018	0.007	0.013	0.016	-0.236
Syndicate	0.002	-0.001	0.009	0.007	0.007	0.013	0.011	-0.145	0.001	0.001	0.004	0.003	0.005	0.001
Union	0.002	-0.002	0.010	0.004	0.001	0.009	0.003	0.032	-1.217	-0.001	-0.009	-0.001	0.000	-0.001
Sanderson	0.001	-0.003	0.007	0.002	-0.002	0.007	0.005	0.013	0.142	-0.975	0.008	0.002	0.004	0.001
Rt 73	0.003	0.000	0.020	0.003	0.000	0.007	0.000	0.072	0.046	0.118	-2.169	-0.026	-0.030	-0.010
RR 228	0.001	-0.003	0.005	0.001	-0.003	0.006	-0.002	0.001	0.002	0.002	0.006	-1.430	0.090	0.089
LW	0.001	-0.003	0.005	0.001	-0.003	0.006	-0.002	0.001	0.002	0.003	0.017	-0.239	-1.581	-0.286
RR 229	0.001	-0.003	0.005	0.001	-0.003	0.006	-0.002	0.002	0.002	0.002	0.008	-0.057	-0.052	-0.993

Table 7.13: Q25 velocity impact matrix.

Δ Peak Velocity Q25 (fps)		Impact on Bridge													
		Gorham	RR 215	Depot	RR 219	Kendall	Hammond	RR 220	Syndicate	Union	Sanderson	Rt 73	RR 228	LW	RR 229
Existing		4.729	5.268	2.323	4.472	6.408	5.154	5.332	3.432	3.795	4.726	3.914	4.128	4.553	3.070
Removed Bridge	Gorham	-0.705	-0.002	0.003	0.000	0.004	0.007	0.000	0.003	0.001	0.003	0.001	0.002	0.001	0.000
	RR 215	0.254	-2.639	-0.030	-0.033	-0.046	-0.036	-0.024	-0.003	-0.009	-0.007	-0.004	0.005	0.003	0.003
	Depot	0.018	0.037	-0.330	-0.002	0.001	0.005	-0.002	-0.006	0.000	0.002	0.000	0.001	-0.001	-0.001
	RR 219	0.050	0.105	0.014	-0.384	0.024	0.042	0.025	0.018	0.010	0.016	0.005	0.008	0.007	0.001
	Kendall	0.011	0.004	0.003	0.010	-0.368	-0.009	0.003	0.004	0.002	0.005	0.001	0.003	0.001	0.000
	Hammond	0.012	0.008	0.003	0.009	0.017	-0.467	0.003	0.005	0.002	0.005	0.001	0.002	0.001	0.000
	RR 220	0.012	0.001	0.003	0.031	0.056	0.049	-1.550	-0.090	0.012	0.019	0.005	0.011	0.010	0.001
	Syndicate	0.010	0.001	0.004	0.005	0.012	0.013	0.015	-0.168	0.000	0.004	0.002	0.005	0.003	0.001
	Union	0.009	-0.001	0.002	0.002	0.006	0.009	0.007	0.010	-0.997	0.000	-0.011	0.002	0.001	0.001
	Sanderson	0.009	0.000	0.003	0.000	0.004	0.007	0.004	0.005	0.143	-0.886	0.006	0.007	0.006	0.003
	Rt 73	0.010	0.004	0.014	0.001	0.007	0.009	0.001	0.061	0.046	0.117	-2.107	-0.027	-0.030	-0.005
	RR 228	0.009	0.000	0.003	0.000	0.004	0.007	0.000	0.003	0.001	0.004	0.002	-1.256	0.105	0.067
	LW	0.009	0.000	0.003	0.000	0.004	0.007	0.000	0.003	0.001	0.004	0.004	-0.191	-1.439	-0.305
	RR 229	0.009	0.000	0.003	0.000	0.004	0.007	0.000	0.005	0.001	0.004	0.000	-0.048	-0.057	-0.708

Table 7.14: TS Irene velocity impact matrix.

Δ Peak Velocity Irene (fps)		Impact on Bridge													
		Gorham	RR 215	Depot	RR 219	Kendall	Hammond	RR 220	Syndicate	Union	Sanderson	Rt 73	RR 228	LW	RR 229
Existing		5.786	8.367	3.858	5.492	7.989	6.519	6.618	4.390	4.403	5.417	4.206	4.669	5.191	3.488
Removed Bridge	Gorham	-0.930	0.004	0.002	0.000	0.000	0.010	0.000	0.003	0.005	0.002	0.000	0.000	0.003	0.002
	RR 215	0.422	-3.634	0.069	-0.050	-0.082	-0.061	-0.030	0.000	-0.028	-0.010	-0.003	-0.003	-0.001	0.004
	Depot	0.009	0.052	-0.653	-0.002	-0.003	0.008	-0.001	0.002	0.004	0.002	0.002	0.000	0.004	0.003
	RR 219	0.013	0.003	-0.001	-0.577	0.061	0.088	0.037	0.023	0.036	0.017	0.008	0.007	0.012	0.005
	Kendall	0.004	0.000	0.001	0.021	-0.580	-0.015	0.005	0.004	0.008	0.004	0.001	0.001	0.004	0.002
	Hammond	0.005	0.000	0.001	0.015	0.023	-0.707	0.002	0.003	0.007	0.003	0.001	0.000	0.004	0.002
	RR 220	0.004	0.001	0.001	0.038	0.061	0.065	-1.954	-0.067	0.031	0.025	0.009	0.012	0.020	0.007
	Syndicate	0.004	0.002	0.002	0.006	0.011	0.020	0.015	-0.294	0.002	0.002	0.003	0.001	0.005	0.860
	Union	0.004	0.001	0.001	0.001	0.002	0.012	0.007	0.038	-1.106	-0.002	-0.012	-0.001	0.002	0.002
	Sanderson	0.004	0.000	0.001	0.000	0.000	0.010	0.002	0.002	0.098	-1.058	-0.010	0.002	0.006	0.006
	Rt 73	0.004	0.000	0.001	0.000	0.001	0.010	0.001	0.007	0.053	0.134	-2.137	-0.019	-0.023	-0.001
	RR 228	0.004	0.000	0.001	0.000	0.000	0.010	0.000	0.002	0.005	0.002	0.001	-1.498	0.073	0.127
	LW	0.004	0.000	0.001	0.000	0.000	0.010	0.000	0.002	0.005	0.001	-0.014	-0.086	-1.577	-0.289
	RR 229	0.004	0.000	0.001	0.000	0.000	0.010	0.000	0.003	0.005	0.001	-0.016	0.035	0.081	-1.187